International Conference on Case Histories in Geotechnical Engineering

(2013) - Seventh International Conference on Case Histories in Geotechnical Engineering

03 May 2013, 2:05 pm - 2:25 pm

Earthquake Geotechnical Engineering Aspects of the 2012 Emilia-Romagna Earthquake (Italy)

Vincenzo Fioravante
University of Ferrara, Italy

Daniela Giretti
University of Ferrara, Italy

Glenda Abate
University of Ferrara, Italy

Stefano Aversa
Università Parthenope, Italy

Daniela Boldini
University of Bologna, Italy

Follow this and additional works at: https://scholarsmine.mst.edu/icchge

Part of the Geotechnical Engineering Commons

See next page for additional authors

Recommended Citation

Author

Vincenzo Fioravante, Daniela Giretti, Glenda Abate, Stefano Aversa, Daniela Boldini, Piera Paola Capilleri, Antonio Cavallaro, Deepak Chamlagain, Teresa Crespellani, Francesca Dezi, Johann Facciorusso, Alessandro Ghinelli, Salvatore Grasso, Giuseppe Lanzo, Claudia Madiai, Maria Rosella Maugeri, Michele Maugeri, Alessandro Pagliaroli, Carlo Rainieri, Giuseppe Tropeano, Filippo Santucci De Magistris, Stefania Sica, Francesco Silvestri, and Giovanni Vannucchi

Commemorate the
Legacy of Ralph B. Peck

Seventh
International Conference on
Case Histories in
Geotechnical Engineering

April 29 - May 4, 2013 CHICAGO

and Symposium in Honor of Clyde Baker

EARTHQUAKE GEOTECHNICAL ENGINEERING ASPECTS OF THE 2012 EMILIA-ROMAGNA EARTHQUAKE (ITALY)

Fioravante Vincenzo
University of Ferrara
Ferrara, (Italy)

Giretti Daniela
University of Ferrara
Ferrara, (Italy)

Abate Glenda
University of Ferrara
Ferrara, (Italy)

Aversa Stefano
Università Parthenope
Naples (Italy)

Boldini Daniela
University of Bologna
Bologna, (Italy)

Capilleri Piera Paola
University of Catania
Catania, (Italy)

Cavallaro Antonio
CNR-IBAM
Catania (Italy)

Chamlagain Deepak
University of Tribhuvan
Kathmandu, (Nepal)

Crespellani Teresa
University of Florence
Florence, (Italy)

Dezi Francesca
University of Camerino
San Marino Republic

Facciorusso Johann
University of Florence
Florence, (Italy)

Ghinelli Alessandro
University of Florence
Florence, (Italy)

Grasso Salvatore
University of Catania
Catania, (Italy)

Lanzo Giuseppe
University La Sapienza
Rome, (Italy)

Madiai Claudia
University of Florence
Florence, (Italy)

Massimino Maria Rossella
University of Catania
Catania, (Italy)

Maugeri Michele
University of Catania
Catania, (Italy)

Pagliaroli Alessandro
University of La Sapienza
Rome, (Italy)

Rainieri Carlo
University of Molise
Campobasso, (Italy)

Tropeano Giuseppe
University of Cagliari
Cagliari, (Italy)

Santucci De Magistris Filippo
University of Molise
Campobasso, (Italy)

Sica Stefania
University of Sannio
Benevento, (Italy)

Silvestri Francesco
University Federico II
Naples, (Italy)

Vannucchi Giovanni
University of Florence
Florence, (Italy)

ABSTRACT

On May 20, 2012 an earthquake of magnitude M_L=5.9 struck the Emilia Romagna Region of Italy and a little portion of Lombardia Region. Successive earthquakes occurred on May 29, 2012 with M_L=5.8 and M_L=5.3. The earthquakes caused 27 deaths, of which 13 on industrial buildings. The damage was considerable. 12,000 buildings were severely damaged; big damages occurred also to monuments and cultural heritage of Italy, causing the collapse of 147 campaniles. The damage is estimated in about 5-6 billions of euro. To the damage caused to people and buildings, must be summed the indirect damage due to loss of industrial production and to the impossibility to operate for several months. The indirect damage could be bigger than the direct damage caused by the earthquake. The resilience of the damaged cities to the damage to the industrial buildings and the lifelines was good enough, because some industries built a smart campus to start again to operate in less of one month and structural and geotechnical guidelines were edited to start with the recovering the damage industrial buildings. In the paper a damage survey is presented and linked with the ground effects. Among these, soil amplification and liquefaction phenomena are analyzed, basing on the soil properties evaluation by field and laboratory tests. Particular emphasis is devoted to the damaged suffered by the industrial buildings and to the aspects of the remedial work linked with the shallow foundation inadequacy and to the liquefaction mitigation effects.

INTRODUCTION

The 2012 Emilia Romagna seismic sequence was characterised by many shocks moving from east towards west, with the main shocks occurred on May 20 (M_L=5.9) and May 29 (M_L=5.8 and M_L=5.3). The macroseismic survey shows heavy damage in spite of the moderate magnitude mainly due to the fact that the Emilia Romagna Region was declared

seismic area starting from 2003. The earthquakes caused 27 deaths, of which 13 on industrial buildings. The damage was considerable. 12,000 buildings were severely damaged; big damages occurred also to monuments and cultural heritage of Italy, causing the collapse of 147 campaniles.

The damage is estimated in about 5-6 billions of euro. To the damage caused to people and buildings, must be summed the indirect damage due to loss of industrial production and to the impossibility to operate for several months. The indirect damage could be bigger than the direct damage caused by the earthquake. It is important to stress that the industrial buildings, built after that the Region was declared seismic area in 2003, were practically not suffered any damage, even if the recorded acceleration was greater than that predicted by the Italian Regulation (NTC, 2008), equal to 0.10-0.15g with a probability of occurrence less than 10% in 50 years. Particularly the vertical accelerations were very high because of the normal fault type and because of many towns were located in the epicentral area.

The geotechnical aspects play a significant role as in the case of 2009 Abruzzo earthquake (Monaco et al., 2012), in terms of site amplification (Maugeri et al., 2011) and liquefaction phenomena (Monaco et al., 2011).

The resilience of the damaged cities to the damage to the industrial buildings and the lifelines was good enough, because some industries built a smart campus to start again to operate in less of one month and structural and geotechnical guidelines were edited to start with the recovering the damaged industrial buildings. In the paper the ground motion is analysed; the soil properties have been investigated for preliminary site response analysis. Particular emphasis is devoted to the damage suffered by the industrial buildings and to the aspects of the remedial work linked with the shallow foundation inadequacy and to the liquefaction mitigation effects.

To this aim, Structural Guidelines (WG-RELUIS, 2012) were edited, as well as Geotechnical Guidelines (WG-AGI, 2012) for retrofitting the shallow foundation of industrial buildings and/or for mitigating the occurrence of liquefaction. The guidelines were devoted to the immediate repairing for operative activities and to the remedial works for upgrading the performance of the building to resist to an acceleration equal to 60% to that predicted by the Italian Regulation (NTC, 2008).

GROUND MOTION

The seismic sequence that struck the area between Emilia-Romagna, Lombardia and Veneto regions in May-June 2012 was characterized by two main events (May 20 and 29) with magnitudes slightly less than M_L 6.0, five more shocks with M_L >5.0, and about 2,500 smaller earthquakes. The area is located south of the Po Plain, in the foreland basin of two mountain chains constituted by the Alps and the northern Apennine. Under thick sedimentary fills along the northern and southern margins of the Po Plain, complex systems of tectonic structures are buried. Due to the fast sedimentation rates and comparatively low tectonic rates, the thrusts are

generally buried and there is little surface evidence of their activity (Toscani et al., 2009).

Before 2012 the information available on the historical seismicity of the area was very poor. The most important earthquake activity, known for the zone at hand, dates back to the year 1570 when a complex and long (almost 4 years) seismic sequence (M_W 5.4), caused severe damage in the city of Ferrara and the surrounding villages. Very recent studies carried out by Castelli et al. (2012), retrieved the traces of several damaging earthquakes that occurred between the 1600s and 1700s; they have been overlooked by the seismological literature and not inserted in parametric catalogues, essentially because the highest macro-seismic effects occurred in circumscribed, mostly rural, areas rather than in big cities.

Three interesting earthquake sequences have been re-evaluated after the seismic event of 2012:

- April 6, 1639, with epicentre between Finale Emilia and Carpi, which caused houses and chimneys to collapse in Finale;
- December 15, 1761 with epicentre between Mirandola, Carpi, Modena;
- May 11, 1778 (Rovereto sulla Secchia, Concordia sulla Secchia, Carpi). This appears to have been a seismic sequence of some duration. The main shock on May 11, 1778, caused irreparable damage to the "most ancient and strong" tower of the Sacchella, located in the nearby village of Rovereto sulla Secchia, which consequently had to be completely demolished (Castelli et al., 2012).

This new information allowed to update the historical seismicity of the area, as shown in Figure 1.

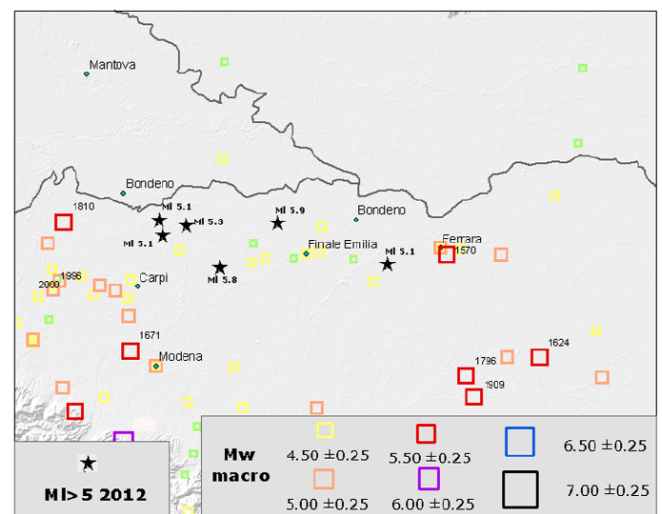*Figure 1. Historical seismicity of the area (Castelli et al. 2012) (data source: Rovida et al. 2011).*

The May 20, 2012, earthquake (M_L 5.9, M_W 6.1) occurred nearly 30 km WNW of the town of Ferrara and east of the Mirandola municipality (in the Modena Province). This event was preceded by a M_L 4.1 event on May 19, 2012 and then followed by four aftershocks. From May 19 to 23, 2012, the

seismic sequence covered an epicentral area extending to the WNW-ESE direction for a length of about 25 km and a width of 10 km, from north of San Felice sul Panaro to Mirabello. Since May 24 to 28, 2012, the area extended further westwards for about 15 km, towards Novi di Modena. Shakemaps derived from the instrumental records provided a quick estimate of the spatial distribution and evolution of ground motion.

In Figures 2 and 3 the instrumental intensity and the PGA maps of the main shocks of May 20 and 29, 2012 are respectively shown.

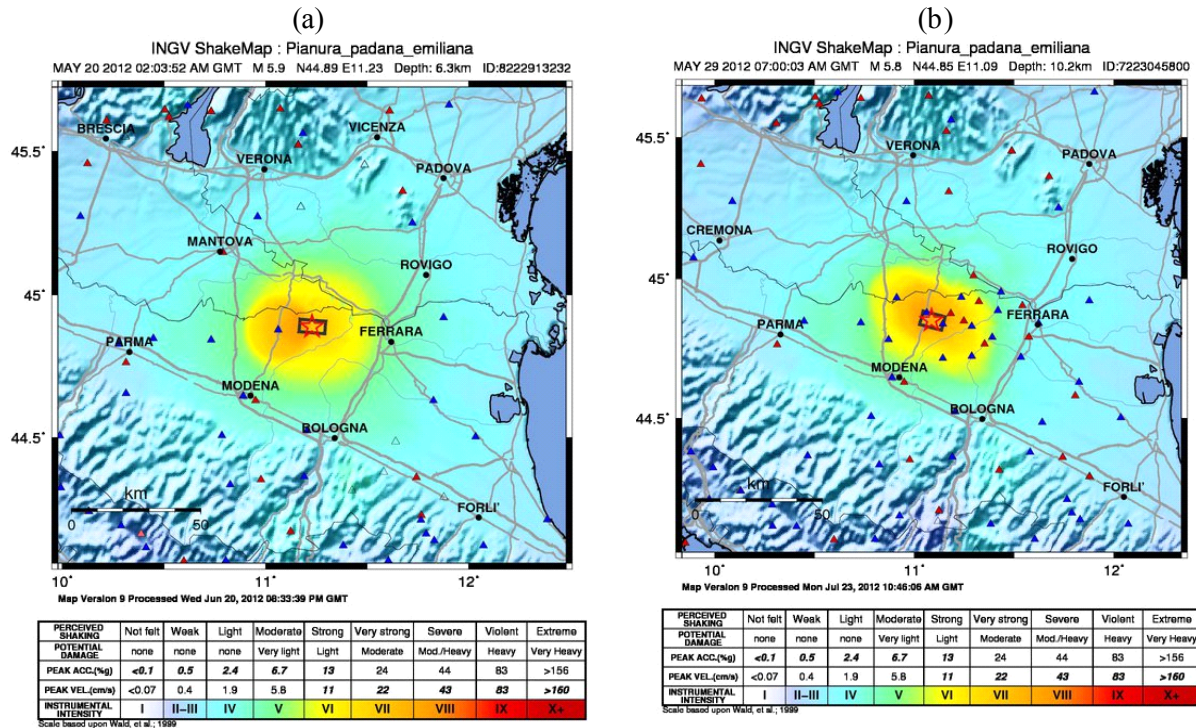*Figure 2. Shakemaps of the instrumental intensity of the main shocks occurred on (a) May 20, 2012 and (b) May, 29, 2012 (http://shakemap.rm.ingv.it/shake/index.html)*
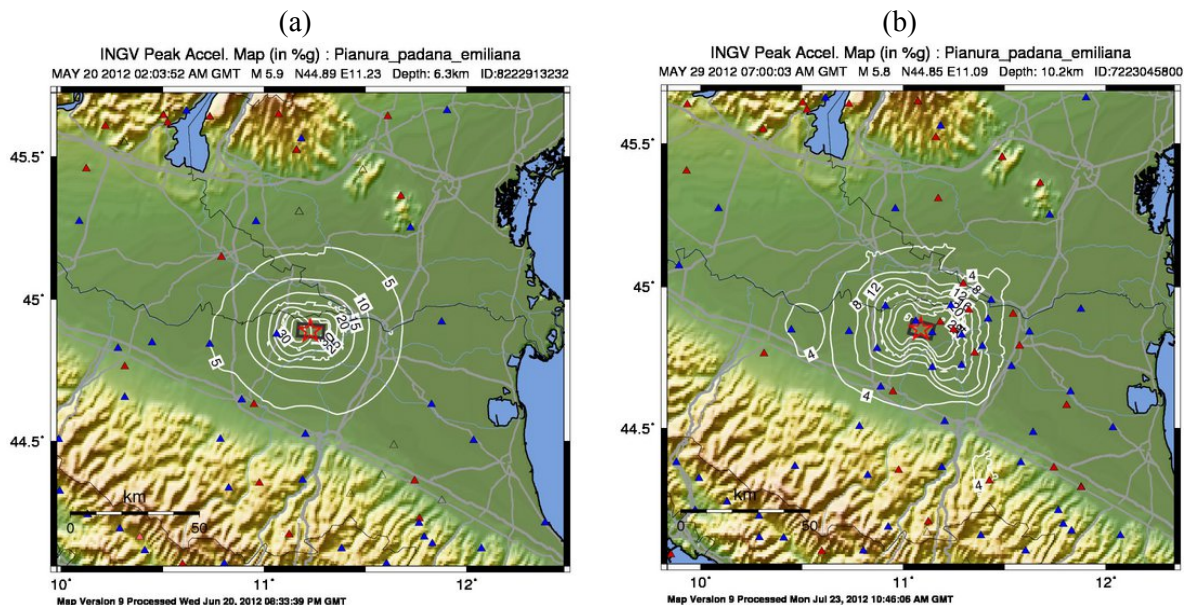

Figure 3.2 – Shakemaps of the horizontal PGA of the main shocks occurred on (a) May 20, 2012 and (b) May, 29, 2012 (http://shakemap.rm.ingv.it/shake/index.html)

In both cases an instrumental intensity between grade VII and VIII may be identified, with a horizontal PGA not higher than 0.32 g (Mirandola MRN station, May 20, 2012), and a PGV up to 54 cm/s.

The Emilia seismic sequence was recorded by a number of stations of the Italian Strong Motion Network (RAN), owned and maintained by the Department of Civil Protection (DPC), and by the Strong Motion Network in Northern Italy (RAIS), managed by the Italian Institute for Geophysics and Volcanology (INGV), Milano-Padova section. After the earthquake of May 20, 2012, in order to increase the density of instruments in the epicentral area, the DPC installed 17 digital stations from May 20 to June 6 (WG-DPC [2012]), most of which recorded the May 29 seismic event.

A complete list of the stations that recorded the earthquakes along with some attributes of the stations and the recording motions can be found Chioccarelli et al. (2012a) and (2012b), and Liberatore et al. (2012). With the aim of comparing the Emilia strong motion records with empirical predictions from recent GMPEs, in this study we have considered the recordings of 37 accelerometric stations located within 100 km from the epicentre of 20/05/2012 earthquake. Details on the subsoil conditions, named A, B, C, according to the Italian Regulation (NTC 2008), and main ground motion parameters

of the considered ground motions are listed in Table 1. The subsoil classification of the stations was derived from Italian seismic database ITACA. The EC8 (2003) subsoil categories were seldom determined on the basis of shear wave velocity profiles, but most times (stations marked with *) only assumed from geological information. Note that most of the stations are located on stiff (class B) to soft (class C) and even very soft (class D) soils, and that the class A (rock outcrop) station closest to the epicentre is as far as 56 km, which implies that the interpretation of seismic records in terms of reference ground motion is rather more complex than usual.

To evaluate the ground motion distribution and the site effects from the digital records of Emilia main shock event, the main parameters calculated from the accelerometric data were compared with those ground motion parameters predicted by Italian attenuation laws for subsoil class A.

The accelerograms were clustered according to the subsoil classes, obtaining 12 records for outcropping rock (A*), 6 records for stiff soil (B*), 18 records for soft soil (C and C*) and 1 record for very soft soil (D). The horizontal components of the selected records have been processed by tapering, correction of baseline and linear trend, and frequency band-pass filtering between 0.1 and 25 Hz.

Table 1. Subsoil classification and epicentral distance of the RAN and INGV stations and main ground motion parameters of the horizontal components.

			Località	SOIL CLASS	r epi [km]	mean value PGA [g]	comp.	PGA (g)	D5-95 (s)	IH (cm)	Tm (s)	comp.	PGA (g)	D5-95 (s)	IH (cm)	Tm (s)
RAN	SSU		Sassuolo	A*	56	0.020	WE	0.0223	29.47	7.7	0.56	NS	0.0175	30.3	7.2	0.542
	TGG		Tregnago	A*	75	0.007	WE	0.0091	17.45	0.9	0.152	NS	0.006	25.51	0.8	0.195
	PVF		Pavullo_del_Frignano	A*	71	0.004	WE	0.0029	68.17	3.8	1.488	NS	0.0051	23.59	4.2	1.419
	SMP		San_Marcello_Pistoies	A*	98	0.005	WE	0.0041	24.61	2	0.568	NS	0.0052	19.55	2.9	0.752
	MDG		Modigliana	A*	93	0.010	WE	0.0093	16.79	1.8	0.33	NS	0.011	18.02	2.1	0.353
	MDT		Modigliana (Trebbio)	A*	97	0.009	WE	0.009	25.78	3.9	0.613	NS	0.0082	19.53	3.9	0.54
	MRR		Marradi	A*	97	0.007	WE	0.0064	20.96	1.6	0.319	NS	0.0073	18.46	1.6	0.345
	BSZ		Borgo_San_Lorenzo	A*	98	0.002	WE	0.0016	35.5	0.8	0.839	NS	0.0019	19.49	0.7	0.535
	ISD		Isola_Della_Scala	B*	49	0.015	WE	0.0136	36.75	7.8	0.633	NS	0.0167	50.4	10	0.836
	MRZ		Marzabotto	B*	60	0.003	WE	0.0033	16.7	1.1	0.452	NS	0.0036	36.62	1.6	0.569
	BRH		Brisighella	B*	87	0.013	WE	0.0139	32.09	5	0.518	NS	0.0116	35.69	4.5	0.574
	GAI		Gaino	B*	99	0.018	WE	0.0244	16.03	3.2	0.288	NS	0.014	19.97	2.1	0.261
	CSP		CastelSanPietroTerme	B*	64	0.014	WE	0.0118	36	8.7	1.233	NS	0.0176	42.26	15.6	1.346
	PTV		Pontevico	B*	100	0.011	WE	0.0098	13.26	4.7	0.539	NS	0.0114	38.53	5.8	0.75
	FRN		Fornovo	B*	92	0.008	WE	0.0078	28.76	3.3	0.621					
	MRN		Mirandola	C*	17	0.285	WE	0.2836	5.26	101.4	0.462	NS	0.2872	5.93	155.5	0.667
	ZPP		Zola_Pedrosa_Piana	C*	42	0.019	WE	0.0154	39.57	11.9	0.93	NS	0.023	22.21	20.3	1.016
	MNS		Monselice	C*	57	0.018	WE	0.0183	12.67	1.8	0.176	NS	0.0173	14.97	1.9	0.179
	CPC		Copparo_Coccanile	C*	52	0.029	WE	0.0235	35.6	16.7	0.959	NS	0.0354	26.07	22.8	0.925
	ALF		Alfonsine	C*	78	0.028	WE	0.0307	15.82	14.5	0.775	NS	0.0257	53.42	12.8	0.936
	SRP		Sorbolo	C*	63	0.033	WE	0.0426	13.84	13.9	0.593	NS	0.0253	25.32	9.4	0.561
	MDC		Medicina	C*	56	0.030	WE	0.0239	22.1	12.7	0.839	NS	0.0381	24.92	18.3	0.799
	PAR		Parma	C*	76	0.007	WE	0.0074	25.96	4.6	0.726	NS	0.0059	25.73	3.6	0.697
	MDN		Modena	C	40	0.037	WE	0.0407	24.71	19.4	0.665	NS	0.034	31.01	14.9	0.653
	NVL		Novellara	C	41	0.049	WE	0.0478	14.2	10.2	0.35	NS	0.0508	11.49	9.4	0.334
	FRE1		Firenzuola	C	87	0.008	WE	0.0089	27.44	2.4	0.467	NS	0.0068	23.87	3.4	0.587
	ARG		Argenta	D	56	0.021	WE	0.0246	20.48	13.5	0.848	NS	0.0174	31.43	10.1	0.852
INGV	BRIS		BRISIGHELLA	A*	85.4	0.008	WE	0.0113	49.95	5.5	1.153	NS	0.0063	55.94	6.1	1.209
	SFI		ZOCCA	A*	63.2	0.005	WE	0.004	26.52	3.3	0.93	NS	0.0053	81.02	4.9	1.355
	ZEN8		SAN_ZENO_DI_MONT.	A*	92.1	0.007	WE	0.0069	21.58	0.9	0.246	NS	0.0075	14.16	1.7	0.322
	ZOVE		ZOVENCEDO	A*	65.9	0.016	WE	0.0156	16.44	1.3	0.177	NS	0.0167	17.42	1.6	0.202
	BDI		FAENZA	C*	84.4	0.013	WE	0.0114	79.53	7.6	1.569	NS	0.0155	103.55	10	1.378
	FIR		IMOLA	C*	71.7	0.015	WE	0.014	53.18	7.5	1.367	NS	0.0157	72.72	9	1.651
	MNTV		MANTOVA	C*	45.5	0.021	WE	0.0196	54.14	15.2	0.972	NS	0.0217	45.05	16	0.844
	FIR		NOVI_DI_MODENA	C*	36.6	0.035	WE	0.0299	40.94	16.9	0.893	NS	0.0421	8.31	17.9	0.731
	OPPE		OPPEANO	C*	46.6	0.017	WE	0.0174	38.05	3.7	0.379	NS	0.0175	68.24	4.7	0.538
	SANR		SANDRIGO	C*	88.6	0.024	WE	0.0238	23.24	2.7	0.215	NS	0.0238	25.29	3.6	0.244
	TREG		TREGNAGO	C*	70.5	0.013	WE	0.0083	24.1	1	0.181	NS	0.0194	22.59	1.5	0.218

In Figure 4, the geometrical mean of the two components of peak ground acceleration, PGA, measured for the selected records are compared with an attenuation law developed on purpose, with the general expression:

$$\log PGA = a + bM_w + c \log \left[1 - \left(\frac{r_{epi}}{h_o} \right)^s \right] + \sigma\varepsilon \qquad (1)$$

The coefficients in eq. (1) were calibrated on the basis of multiple regressions of peak acceleration data of class A recordings of Italian earthquakes occurred before 2002, obtaining a=-2.626; b=0.379; c=-0.507; h_0=10 km; ε=3.5 and σ=0.258.

Figures 4b, c and d show similar comparisons in terms of Housner intensity, I_H, mean period, T_m, and significant duration, D_{5-95}, predicted by the attenuation laws by Tropeano et al. (2012) and Tropeano et al. (2009), respectively.

Figure 4a shows that the measured PGA for class A sites (black symbols) is, on the average, lower than the mean trend observed for Italian seismicity, which is more consistent with the average data recorded by class B stations (blue symbols). The PGA recorded by stations on soft soils (green symbols) are most times underestimated by the attenuation law and the unique data point relevant to a very soft soil (red symbol) falls just on the curve, maybe due to non-linear attenuation.
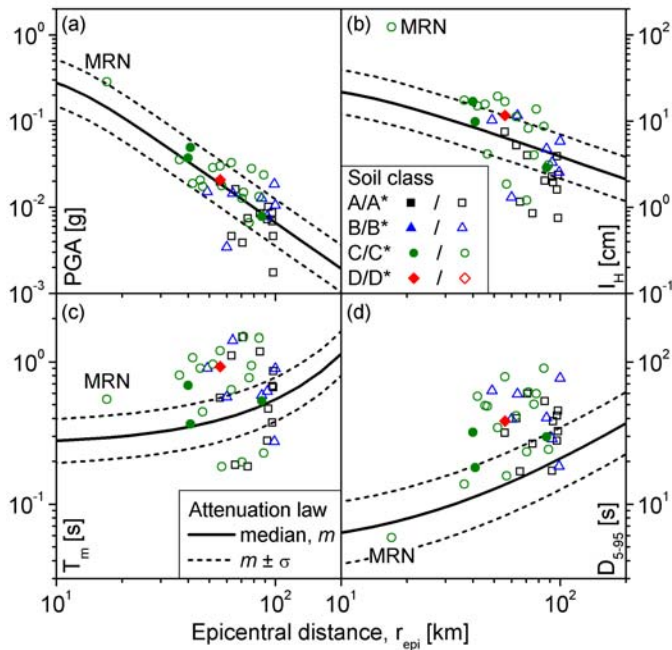

Figure .4. Comparison between peak ground acceleration, PGA (a) Housner intensity, I_H (b), median period, T_m (c) and significant duration, D_{5-95} (d), measured for main-shock of Emilia seismic sequence (May 20, 2012, M_w 6.1) and the reference values predicted by attenuation laws suitable for Italian seismicity.

The site amplification effects are more evident on the ground motion distribution in terms of mean I_H (Figure.4b). In this case, for example, the value measured for Mirandola station (MRN, class C*) exceeds the expected reference value for about 7 times.

The variation of the mean period TM with distance shows a greater scatter (Figure.4c), which appears independent from the subsoil class. On average, the seismic records are characterized by lower frequencies than those predicted by the attenuation law.

The significant duration D_{5-95} is on average twice that expected from the attenuation law (Figure 4d). The unusually high values of period and duration of the whole amount of seismic records confirm that the ground motion was highly affected by significant large-scale (due to alluvial basin reflections) and local (due to the uppermost layering) amplification effects.

In the following, emphasis is especially given to the ground motions recorded within the epicentral area because these data represent a unique opportunity to provide some insights into the ground motion characteristics in the near-field for moderate magnitude earthquakes.

The acceleration and velocity time-histories of the horizontal and vertical components of motion recorded at the MRN station are illustrated in Figures 5 and 6 for the seismic events of May 20 and May 29, respectively.

The measured ground motions are rather high in the near field. For the event of May 20, the MRN station is located to the east of the epicentre at a distance of about 13 km and recorded the highest horizontal peak acceleration of about 0.26g. Both NS and EW components have similar peak accelerations values; vertical PGA is slightly higher than horizontal one, attaining a peak value of 0.31g. As usually observed in the near-field, peak ground velocity (PGV) shows a distinct long-period pulse for both horizontal components of motion: interestingly enough the PGV value of the NS component (47.9 cm/s) is about twice that of the EW component (29.5 cm/s). Same considerations hold for the ground motion recorded at the MRN station for the event of May 29 seismic, located at about 4 km distance from the epicentre.

In this case, however, a much higher value of the peak ground vertical acceleration (0.889g) was measured with respect to the horizontal values (0.224g and 0.295g for the EW and NS, respectively).

As for the May 20 event, higher values of PGV were recorded for the NS component (57.1 cm/s) with respect to the EW one (28.6 cm/s).

The spatial variability of peak ground acceleration may be observed in Figure 7 which reports the horizontal and vertical PGA values measured at several stations within a distance of 30 km from the epicentre of the May 29 earthquake. The PGA values vary significantly, despite the similarity of epicentral distance and soil conditions. At the station of San Felice sul Panaro (SAN0), which is located in the near field about 5 km to the east of the epicenter, the same picture already seen for MRN holds, i.e. vertical PGA values higher than horizontal ones.
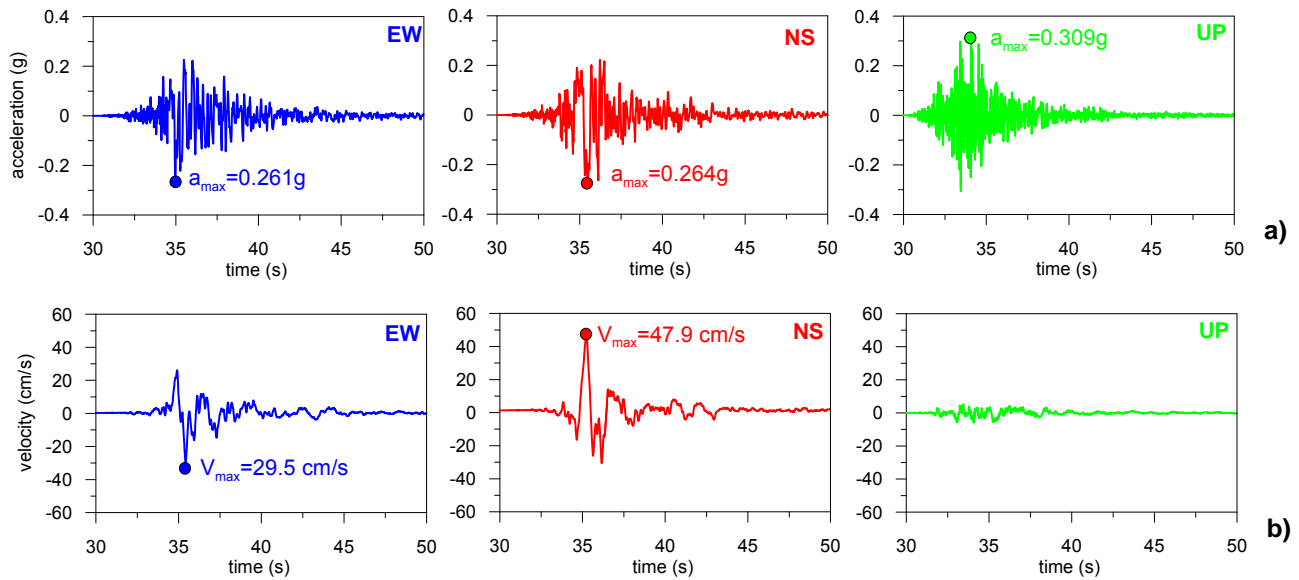
Figure 5. Acceleration (a) and velocity (b) time histories recorded at the Mirandola (MRN) station during the seismic event of May 20, 2012.
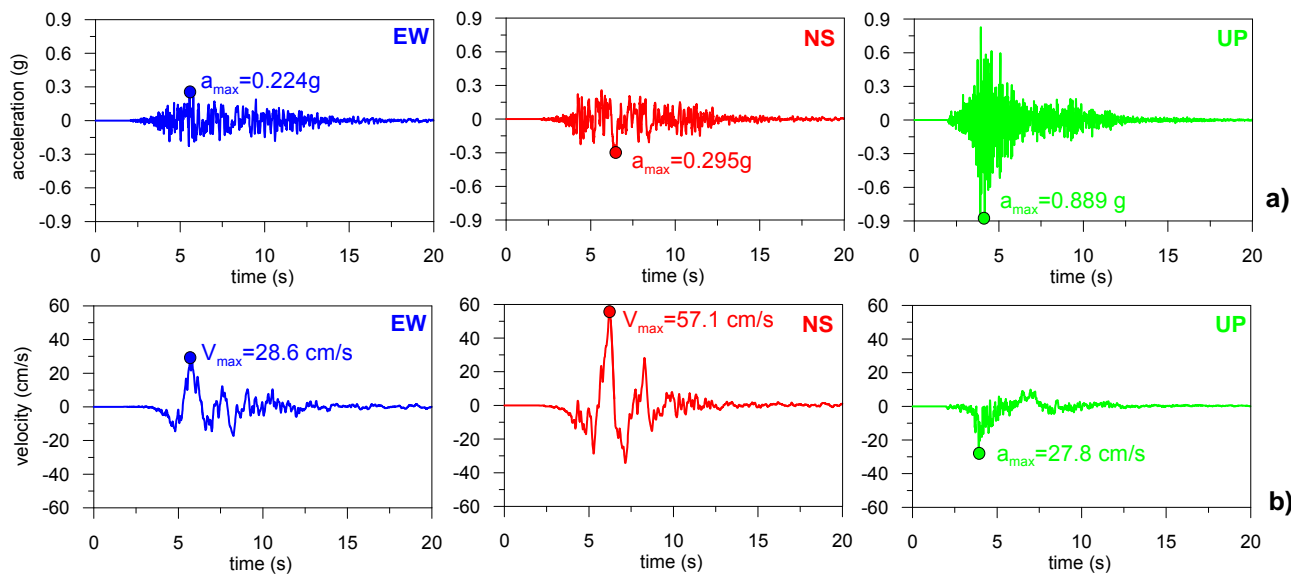

Figure 6. Acceleration (a) and velocity (b) time histories recorded at the Mirandola (MRN) station during the seismic event of May 29, 2012.

The highest horizontal peak acceleration (0.241g) occurred at the Moglia (MOG0) station located about 16 km west of the epicentre. Ground motions recorded at Finale Emilia (FIN0), lying east of the epicentre, shows much larger amplitudes than those at the southern station of Ravarino (RAV0), located at similar distance from the epicentre. It is most likely that a combination of seismological and geological effects may have caused the observed variability of ground motion.

The 5% damped elastic acceleration response spectra of the ground motions recorded at the near-fault stations MRN and SAN0 are plotted in Figure 8 for both horizontal and vertical components.

Very large values of the vertical acceleration at periods of about 0.05 s are observed at all stations and for both events for; slightly more than 3g are reached at the MRN station for the shock of May 29.

However, spectral ordinates of the vertical acceleration decay very rapidly with the vibration period. Comparison of response spectra of horizontal motions indicate that spectral ordinates attain maximum values of about 1g at short periods (0.2-0.6 s) and show some other important peaks at larger periods (1.0-2.0 s). For periods higher than 0.2s the horizontal spectral ordinates are much higher than vertical ones.
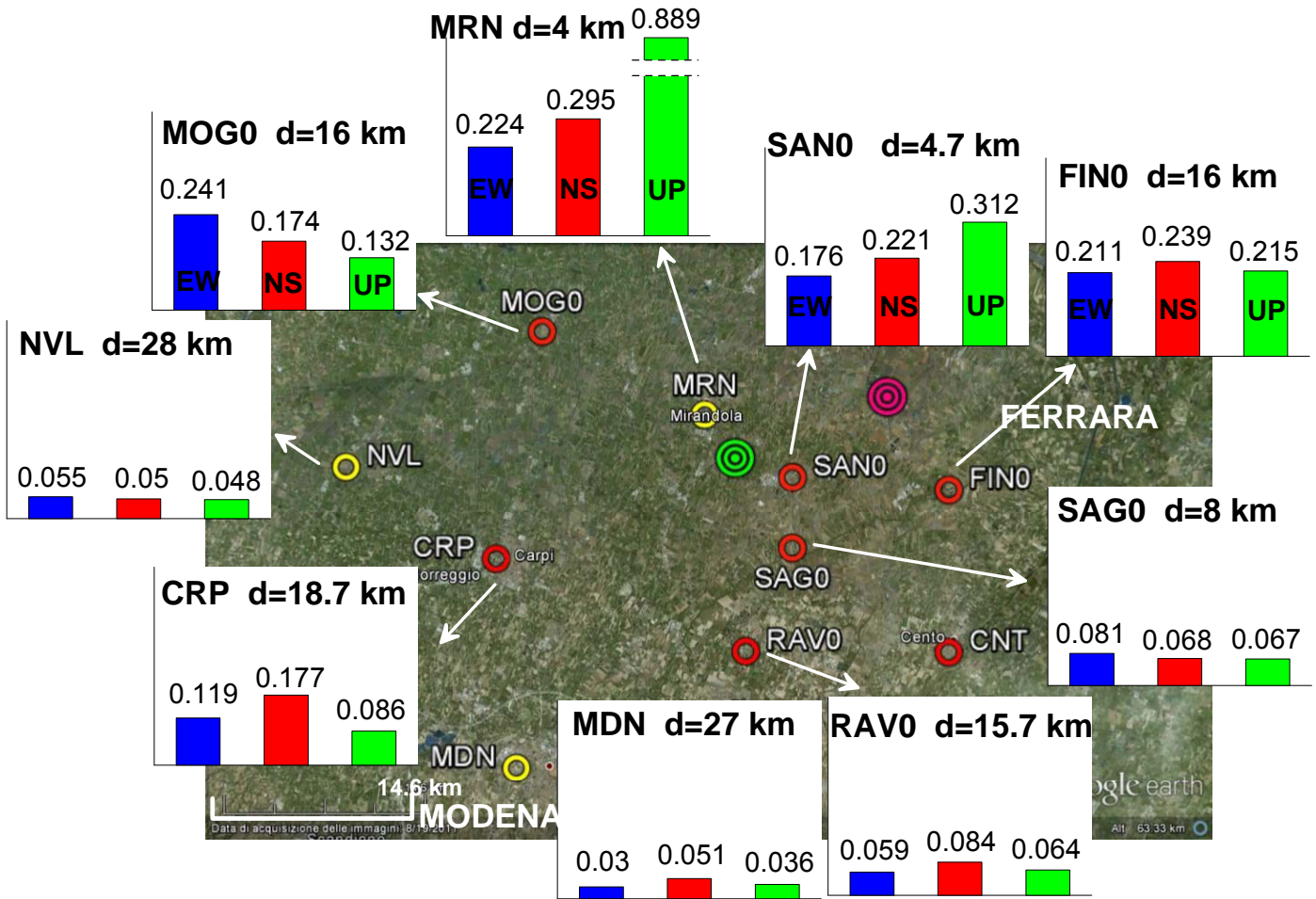
Figure 7- Horizontal and vertical peak ground acceleration values recorded at several stations within a distance of about 30 km from epicentre of the May 29 mainshock (yellow circle= permanent RAN stations; red circle=temporary RAN stations; pink symbol=epicentre of the May 20, 2012 event; green symbol=epicentre of the May 29, 2012, event).
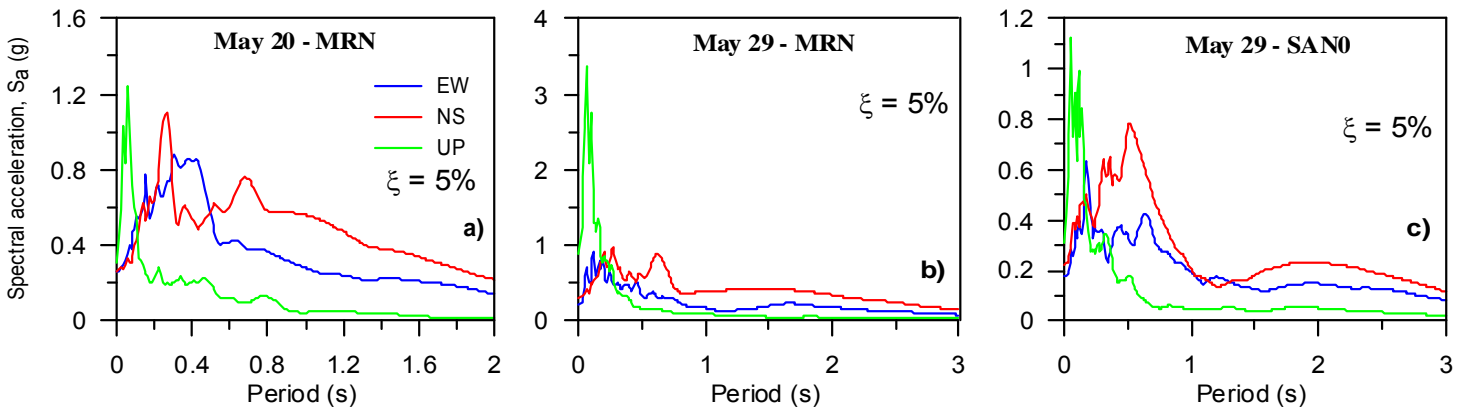

Figure 8. Acceleration response spectra (5% damped) of horizontal and vertical components: (a) MRN station for the seismic events of May 20, 2012 (a) May 29, 2012 (b); SAN0 station during the seismic event of May 29 (c).

To provide further insights into the relative amplitude of the vertical with respect to the horizontal motion into the whole period range, Figure 9 shows the ratio of vertical-to-horizontal response spectra (V/H) as a function of period for both events of May 20 and May 29 at the stations MRN and SAN0. It is confirmed that, as pointed out several times in the literature (see e.g. Bozorgnia and Campbell, 2004; Lanzo and Pagliaroli, 2012), amplitude of the vertical component at short periods overcomes the horizontal one leading to V/H values that may significantly exceed unity in the near-fault region. The commonly assumed rule-of-thumb of a 2/3 ratio between vertical and horizontal PGA is not satisfied for sites close to the fault. Furthermore, it has also been shown that the rule of two-thirds is conservative at long periods.

In more detail, at both stations the V/H ratio is similar for the horizontal components and it generally takes maximum values of about 4 around 0.05 s. Much higher difference between vertical and horizontal ground motion does occur at MRN for the May 29 event for which the V/H ratio attains values up to 8 at about 0.06 s for the NS component. At larger periods (i.e. periods longer than 0.2 s) the V/H ratio generally is lower than 2/3. The observed values at low periods are much higher than those recorded during the 2009 Abruzzo earthquake at several recording stations located in the near-fault on stiff soils (Pacor at al., 2009; Lanzo and Pagliaroli, 2012). Considering that the MRN and SAN0 stations are characterized by much more deformable soils, it can be speculated that part of the observed differences in the V/H ratios may be attributed to the different soil conditions. More investigations are necessary to corroborate this hypothesis. To give some indications on the severity of the near field recorded ground motion with respect to the design requirements, the horizontal and vertical acceleration response spectra of the motions recorded at the MRN station are plotted together with the Italian Building Code NTC08 (NTC, 2008) elastic spectra in Figure 10.
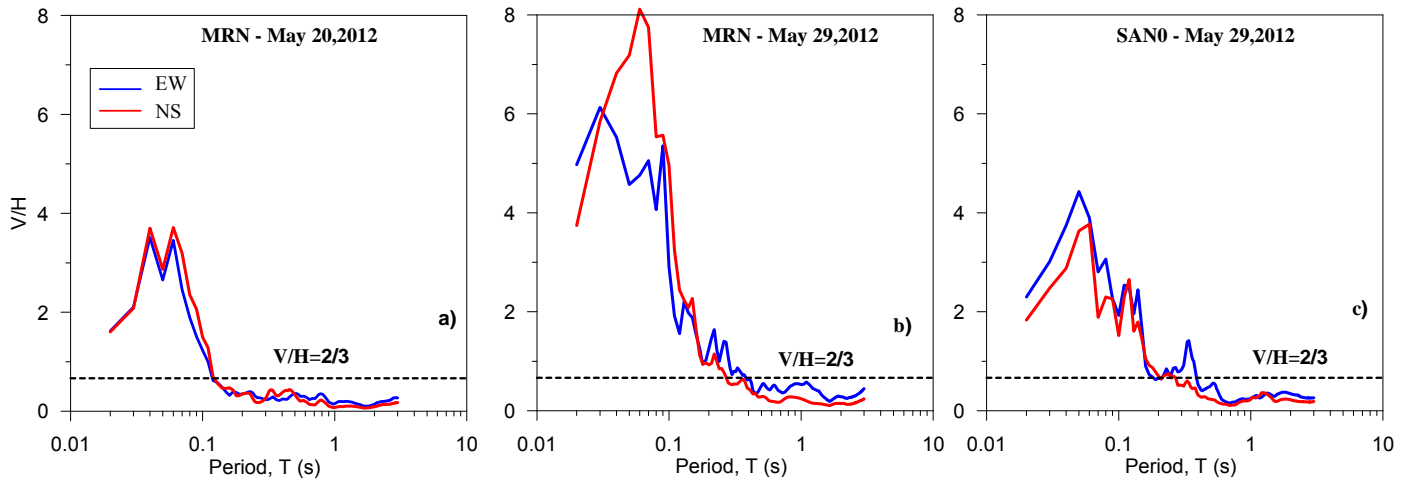

Figure 9. Spectral ratio V/H between the vertical and the horizontal acceleration response spectra (5% damped) at MRN station for : May 20 (a) and May 29 (b) events; (c) SAN0 for the May 29 event.
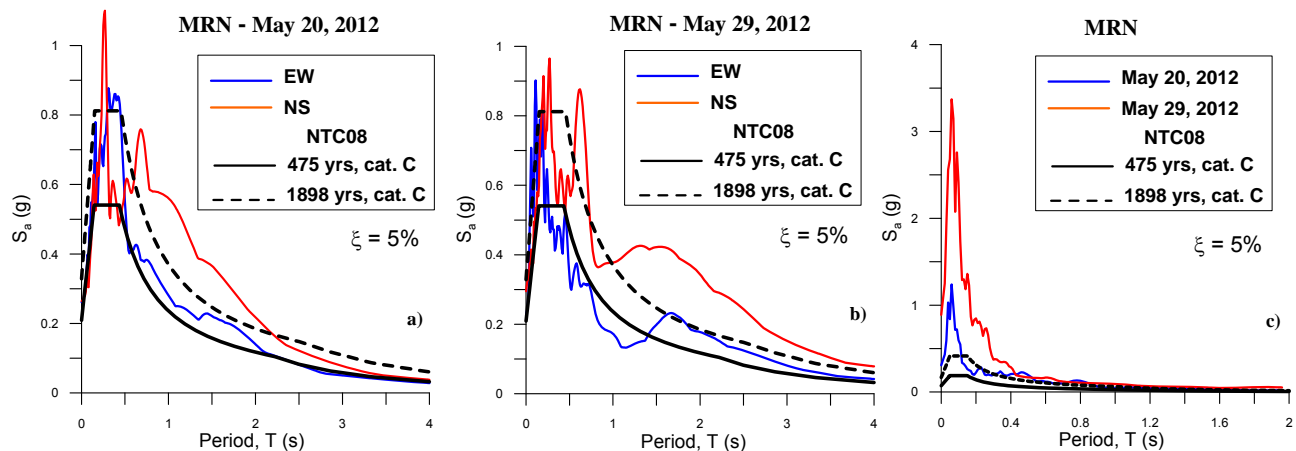

Figure 10. Acceleration response spectra (5% damping) from ground motions recorded at MRN station for: horizontal (a,b) and vertical c) components compared to the Italian Bulding code spectra for 475 and 1898 years return periods.

These latter are presented for two return periods, i.e. Tr=475 years and Tr=1898 years which correspond to the ultimate limit state SLV (life safety) design for ordinary (reference period VR=50 years) and strategic buildings (reference period VR=200 years), respectively. The code spectra are shown for type C subsoil conditions according to which MRN can be classified. For Tr=475 yrs and TR=1898 yrs, the spectra are anchored to the PGA equal to 0.21 g and 0.33g, respectively.

As the horizontal motion is concerned, spectral ordinates of recorded motions are much higher than those considered by the national code over the whole range of periods for ordinary constructions while for strategic buildings only the NS component generally exceed the code spectral ordinates for period longer than 0.6 s (Figure 10a and b). As regards the vertical component (Figure 10c), values significantly larger than those of the codes are observed especially at short periods (i.e. for periods lower than 0.1s); it should be remarked that for the May 29 event recorded spectral accelerations exceed code values up to 0.4s.

GROUND PROPERTIES

The main tectonic structure of the whole area is a buried ridge known as Ferrara Folds, which reaches its maximum height (about 130 m below the ground surface) NW the city of Ferrara under the Po river, near the site of Casaglia.

The subsoil is characterized by alluvial deposits of different depositional environments, which consist in an alternating sequence of silty-clayey layers of alluvial plain and sandy horizons of channel and levees.

These deposits are about 250 m thick and the geological substratum consists of marine and transition deposits of lower-middle Pleistocene age.

Geophysical test results and the values of fundamental frequencies of deposits obtained from ambient vibrations measurements, indicate that the depth of the seismic bedrock is greater than 150 m.

Figure 11 reports an offprint of the geological and geomorphological maps of the areas of interest, where the lithological characteristics of the shallow deposits (Holocene deposits, 10-15 m deep) and the main geomorphological structures present in the western sector of the Ferrara plane are evidenced. The Figure shows that the towns of S. Carlo and Mirabello have been constructed above the abandoned channel of the Reno river and that the sand is the prevailing lithology in the band near this paleo-channel. The ancient banks of the Reno river are still present and they are the areas morphologically most elevated than the surrounding floodplain (altitude difference of 5 – 6 m). The historic cores of towns of S. Carlo and Mirabello are situated right on the banks, in order to safeguard buildings from floods.

To investigate the geotechnical properties of the soils at the sites of S. Carlo and Mirabello, a large series of in situ and laboratory tests and geophysical tests were performed. As an example, at the site of S. Carlo the following in situ tests were performed:

– 10 continuous borings (S) 12 deep with undisturbed samples, equipped with piezometers, both standpipe and vibrating wire;
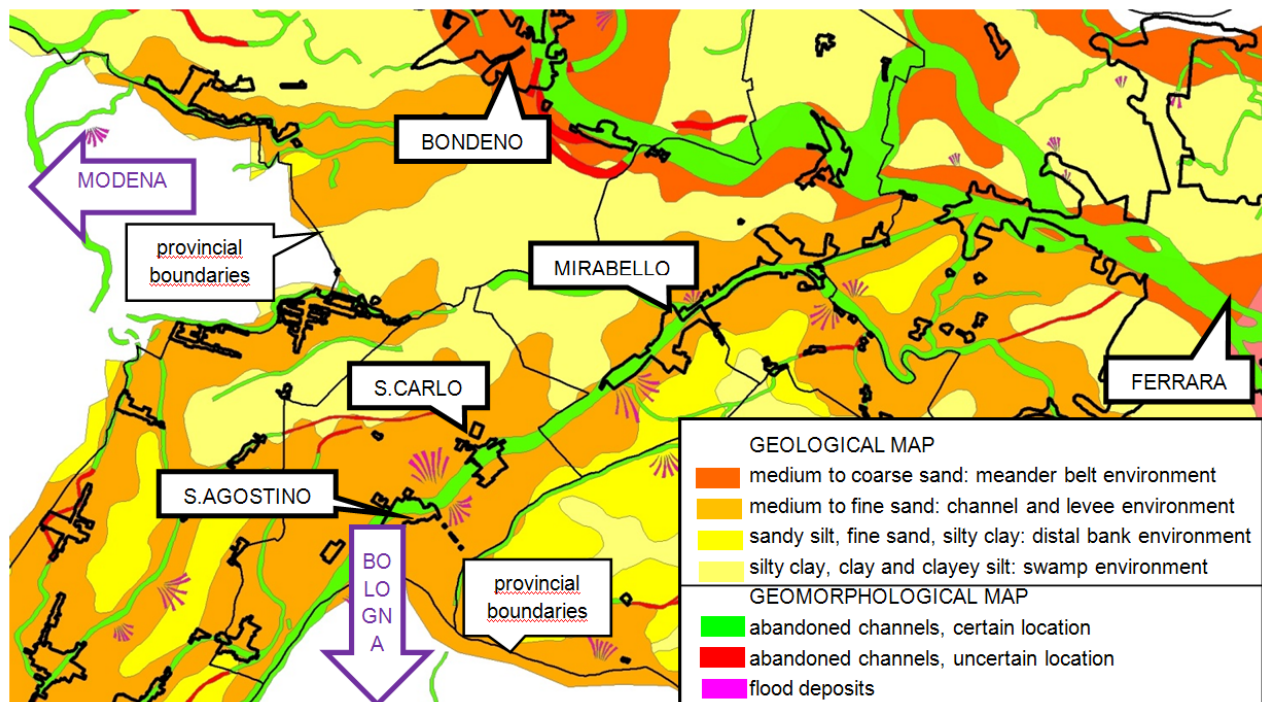

Figure 11. Offprint of the geological (1:250.000) and geomorphological map (1:100.000) of the Ferrara plane.

- 3 destruction borings (SD) 8 m deep, equipped with piezometers, both standpipe and vibrating wire;
- 1 destruction borings 40 m deep equipped for CH test;
- 10 piezocone tests (CPTu) 20 m deep;
- 4 seismic-piezocone tests (SCPTu) 30 m deep.

The stratigraphic sequence evaluated in correspondence of the cross section A-A evidenced in Figure 12 is represented in Figure 13 (the section is drawn across the track of the paleo-channel), where the results of in situ tests along the section are also shown.

The results of the SCPTu tests are reported in Figure 14: the cone resistance qc and the measured shear wave velocity V_S are plotted as a function of the altitude above sea level; Figure 15 reports the grain size characteristics and index properties.
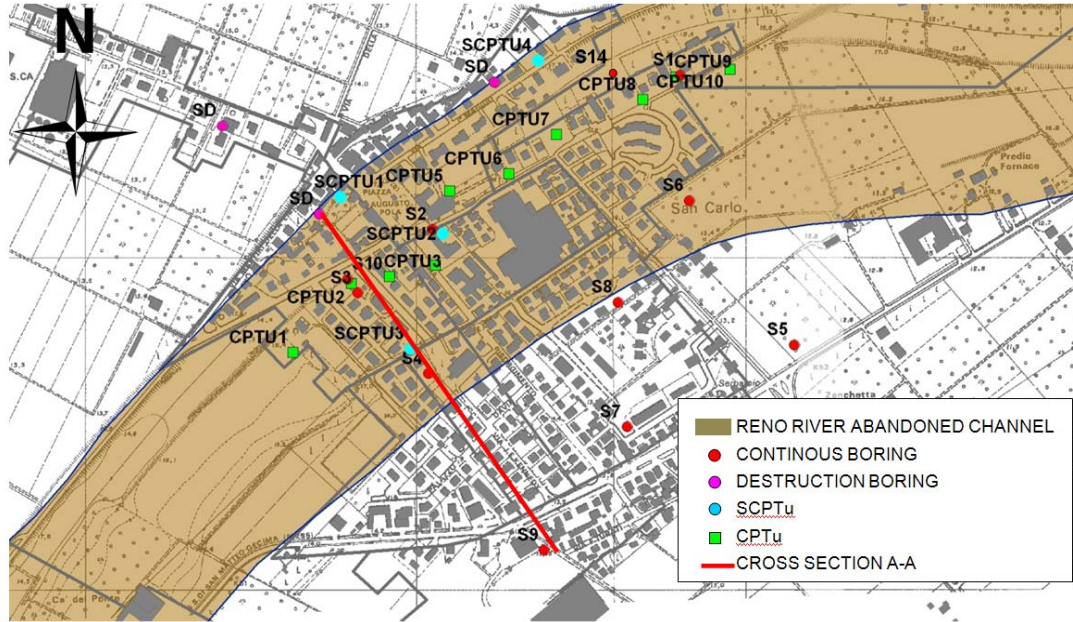
Figure 12. Location of in situ tests in the area of S. Carlo.
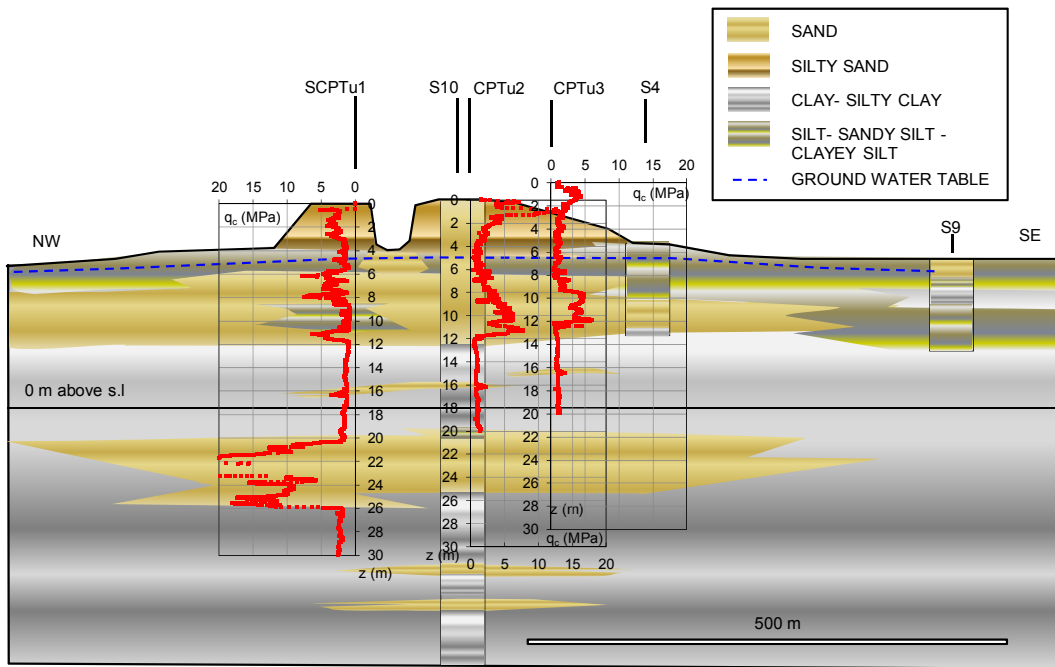
Figure 13. Cross-section A-A: q_c = cone resistance, z = depth below the ground surface.

Figure 14. Seismic-piezocone test results: a) cone resistance qc and b) shear wave velocity V_S profiles.

Figure 15. Grain size characteristics and index properties of the alluvial deposits at S. Carlo, as a function of the altitude above sea level: a) grading, b) mean grain size D_{50}, c) index properties and d) plasticity index.

Figure 16 reports the measured grain size curves of the soils present up to 15-20 m below the ground surface. Figure 17 shows the state parameters of the inves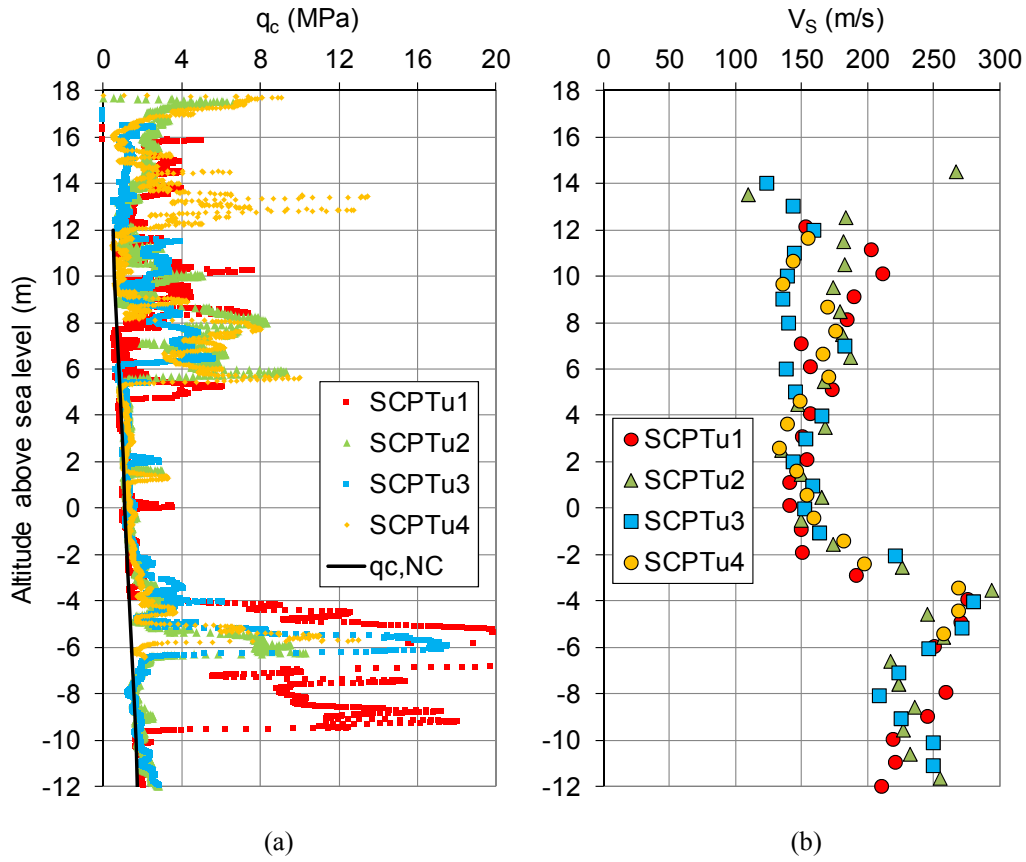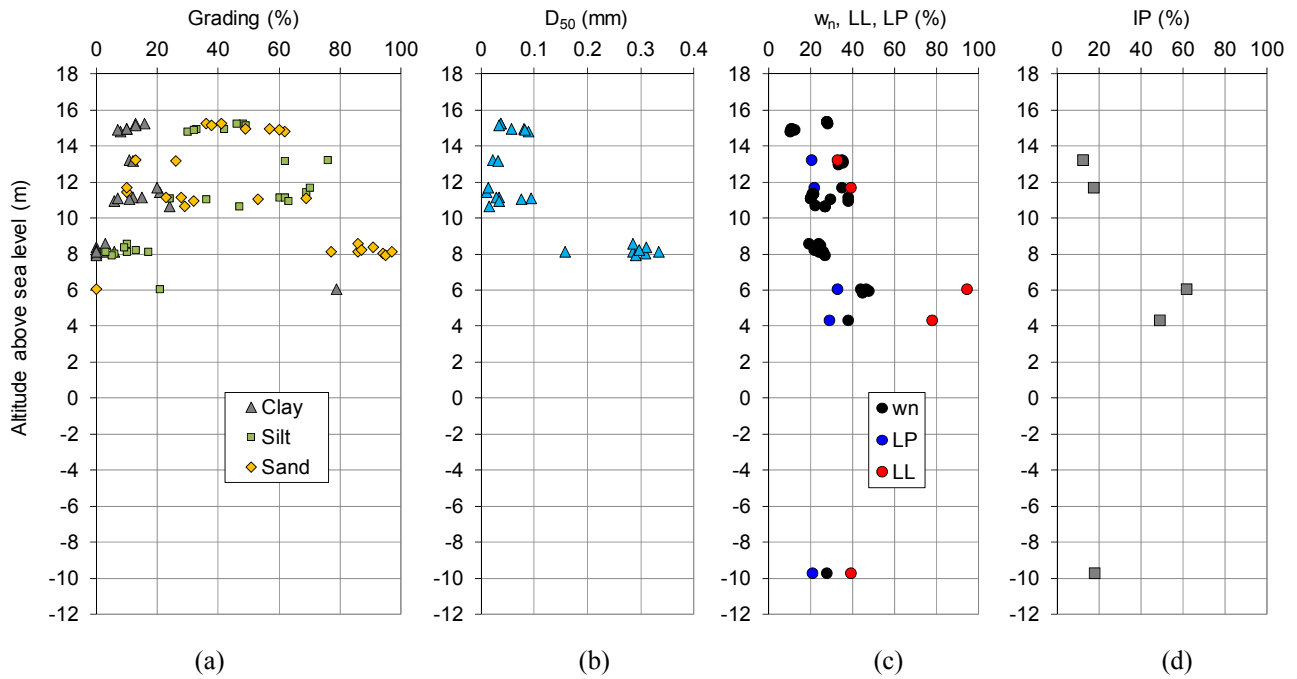tigated soils at San Carlo as a function of the altitude above sea level, in terms of: a) relative density D_R, b) unit weight γ and c) void ratio e. Four main lito-stratigraphic units have been evidenced within the first 20 m below the ground surface.

The banks of the paleo-channel mainly consist of silty sand and fine sand (unit 1); the clay content is lower than 20% and the relative density ranges from 30% to 50%.

Below the banks, a fairly continuous layer, 2 m thick, is present (unit 2), which consists of alternation of sandy silt and clayey-silt of low plasticity. It is followed by a 4-6 m thick layer of medium sand (unit 3), which is the river bed deposit (paleo-channel). The fine content is lower than 15% and the relative density ranges from 30 to 60%.

Unit 3 is followed by a 8 m thick layer of clay and silty clay with local presence of organic fraction (unit 4, deposits of alluvial plane). The base of the clay is the interface between Holocene and Pleistocene deposits; the latter consist of alternating sequence of sandy horizons and silty-clayey layers. The piezometer measures performed during the summer season indicate that the ground water table is about 4-5 m deep from the ground surface in correspondence of the river banks and of 2-3 m deep in the surrounding alluvial plane.

The CPTu and SCPTu test results shown in Figures 13 and 14, indicate that the resistance and stiffness of the first 12 - 13 m (units 1, 2 and 3) are pretty low; in particular the clean sand layer between 7-8 and 11-13 m from the ground surface is characterized by a mean value of the cone resistance qc ≈5 MPa and a mean value of the shear wave velocity VS ≈ 180 m/s.

The clay layer underneath (unit 4) is almost normally consolidated, as shown in Figure 14 where the qc,NC computed for an equivalent normally consolidated clay is shown.
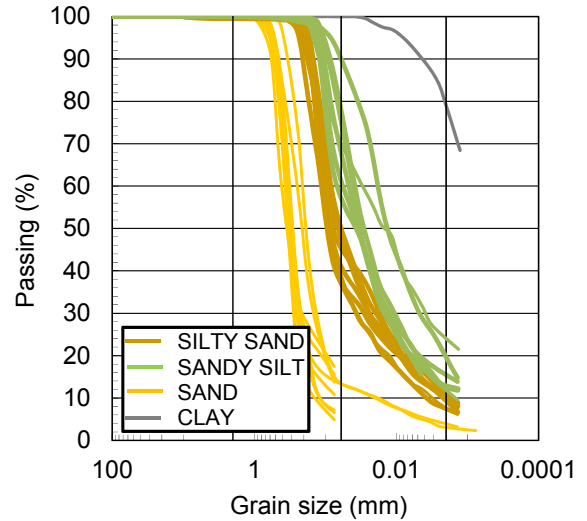
Figure 16. Grain size distributions.

The results of the cone penetration tests have been used to evaluate the relative density D_R and the undrained shear strength c_u of the coarse grained and fine grained layers, respectively, as reported in Figure 18, where the D_R and c_u profiles obtained from the SCPTu tests are plotted as a function of the altitude above sea level.
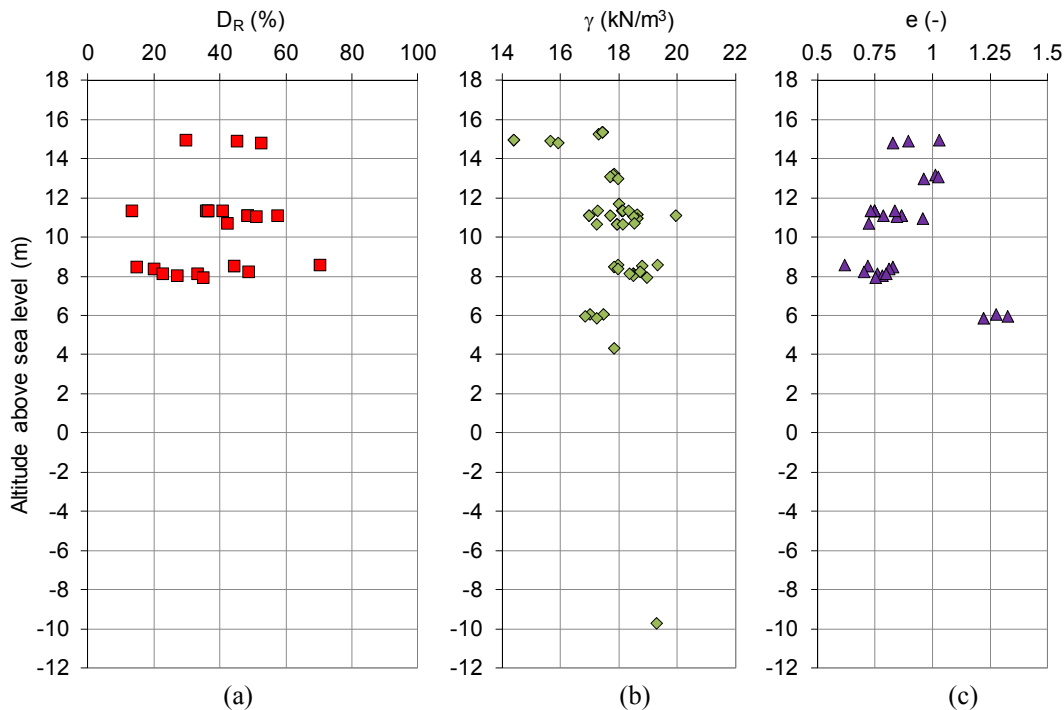
Figure 17. State parameters of the alluvial soil at the site of S. Carlo: a) relative density D_R, b) unit weight γ and c) void ratio e.
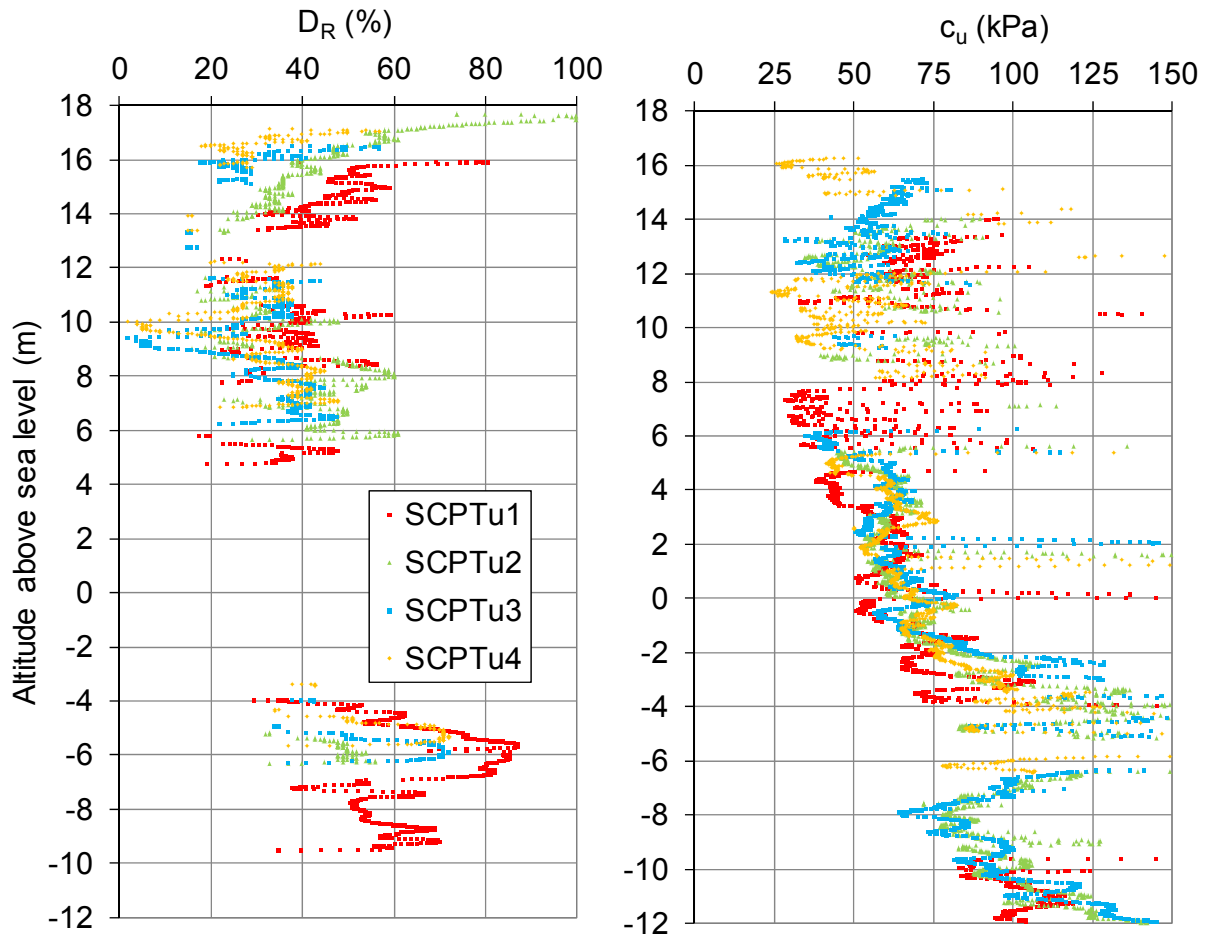
Figure 18. Computed relative density D_R and undrained shear strength c_u from seismic-piezocone tests.

The values of D_R and c_u have been computed using the following equations by Lancellotta (1983):

$$D_R = -98 + 66 \cdot \left[\log \left(\frac{q_c}{\sqrt{\sigma'_{v0}}} \right) \right] \quad (2)$$

$$c_u = (q_c - \sigma_{v0})/N_k \quad (3)$$

where:
σ'_{v0} = vertical effective stress;
q_c = measured cone resistance;
σ'_{v0} = vertical total stress;
N_k = cone factor, assumed equal to 20 (Jamiolkowsi et al. 1982, Lunne et al. 1997).

In accordance with the laboratory determinations, the computed D_R profiles confirm that the shallow sandy layers are characterized by low to medium density.

In Figure 19 are reported the curves representing the dependence of the shear modulus G, damping ratio D and excess pore pressure Δu on the shear strains γ for the units 1, 3 and 4, as deduced from resonant column tests and triaxial test with local measurements (Fioravante et al. 1994). It is very important to note that both the sand and the sandy silt start to develop significant excess pore pressure at very small strains ($\gamma \approx 0.2$-0.4%).

PRELIMINARY SITE RESPONSE

Ground Model
The area struck by the Emilia-Romagna earthquake lies on deep alluvial deposits of the Po Valley, a large basin of Quaternary sedimentation. The inferior Pleistocene sediments consist of sandy clays of marine origin while marine clayey facies and continental sands alternate in the superior Pleistocene. Holocene deposits are of continental origin and are represented by alternating layers of sandy clays, sands, silty sands and peats. The upper strata are constituted by fine graded cohesionless soils (sands and silts) of alluvial recent origin and are spatially heterogeneous (see Figure 20). The water table depth is generally very shallow in the overall area. According to a recent research conducted by Emilia-Romagna Region (Severi and Staffilani, 2012), in springtime the water table level is about 80 to 130 cm below ground surface. Morphology and physical features of the area were visibly shaped by human action, with a lot of works carried out in many centuries for flood defense and marsh reclamation. Since the sixteen century, the interventions were very frequent and extensive: the area is now crossed by many ancient underground drainages, old river beds, reclamation works, and many streams that run along the plain and in some zones get lost into the subsoil.
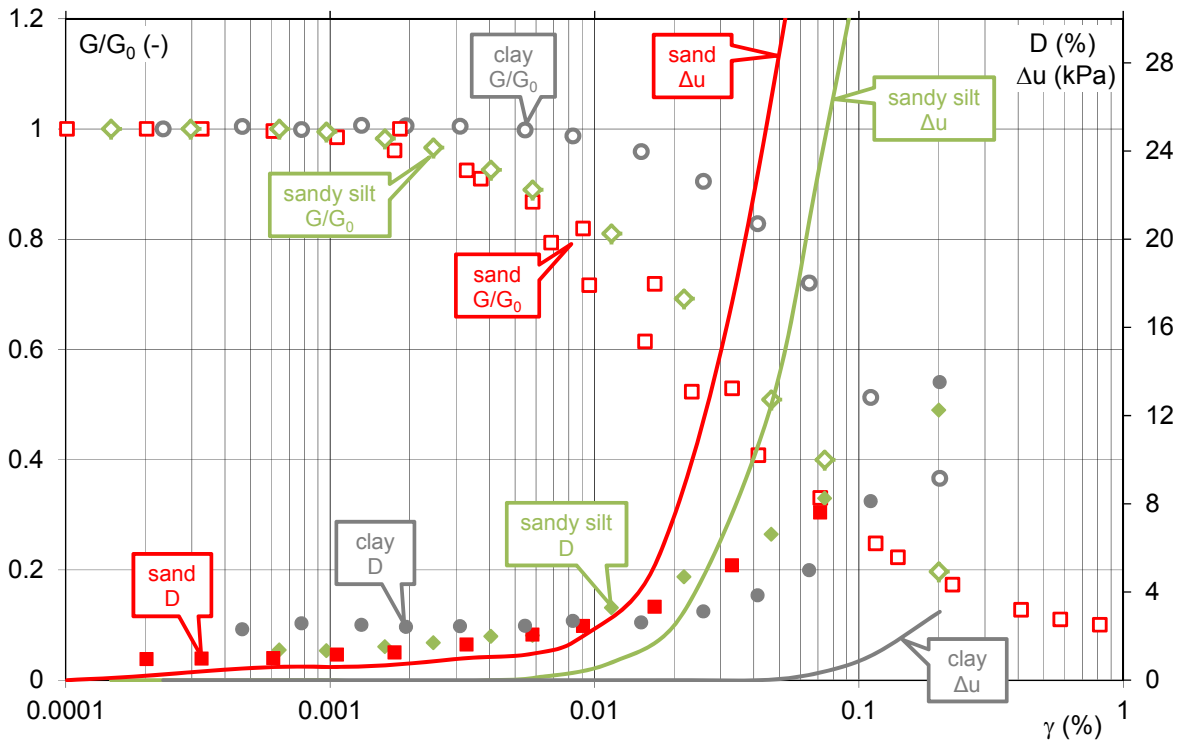
Figure 19. Dependence of the shear modulus, damping ratio and excess pore pressure on the shear strains.

Over time, farming activity settled in the area by occupying natural humps formed by rivers and their abandoned branches, also extending to surrounding areas by means of soil filling. Some historical studies (Cazzola, 1997) indicate that special silts were generally used in filling as they were considered very fertile. In order to promote a more rapid development of the agriculture, many spectacular reclamation works were undertaken in the whole region from the Unity of Italy (1861). Three main types of interventions were performed: filling, drainages, and mechanical water uplifts. In many sites, the stream muddy waters were diverted in zones delimited by natural or artificial embankments, that occupy a large part of the territory. Since 1960, industrial development has been growing and many reclaimed areas were occupied by factories and dwellings. In the subsoil of area under study the following lithologic units are present from top to bottom:

(A) embankment (paleo-levee): about 4 m thick of fine sands alternating with sandy silts

(B) river channel unit (Holocene): 6 to 8 m thick of alternating layers of sandy silts and silty sands

(C) unit of the marshes (Holocene): 5 to 10 m of clays and silts with abundant organic fraction of lacustrine origin

(D) unit of the flood-plain (Pleistocene): sandy silts and silty sands including fine to medium sandy layers and lens

(E) unit of the alluvial plain (Pleistocene): mainly sands

Figure 20 represents some cross sections at San Carlo village showing the typical variability of soil layers.
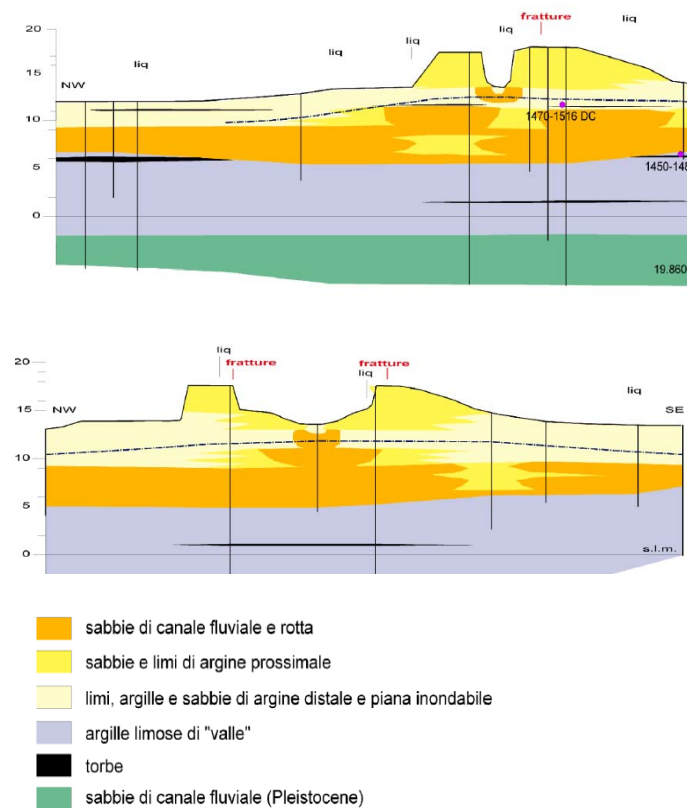

Figure 20. Lithostratigraphic sections across San Carlo village (after Martelli, 2012).

For the geotechnical characterisation of area struck by the earthquake of May 2012 the results of some geotechnical surveys carried out before the earthquake for different purposes and in different times were already available. A lot of information, very different for quality and reliability, were found in the geotechnical data base of the Emilia-Romagna Regional Government (RER-DB), others were derived from geotechnical reports performed for the design of local infrastructures, especially the Cispadana highway (CIS). After the earthquake new and specific in situ and laboratory tests were planned and carried out (WG-DPC). Number, type and source of the tests available at Sant'Agostino and Mirabello are listed in Table 2. The localization of in-situ tests performed by the WG-DPC 2012 are reported in Figure 12.

Table 2 – Number, type and source of the in situ tests available at Sant'Agostino and Mirabello

	BH	CPT	DH
WG-DPC	28	22	10
RER-DB	152	182	
CIS	34	28	5

BH: stratigraphic and/or geotechnical boreholes; CPT: Cone Penetration Tests; DH: Down Hole tests and Seismic CPT

The vertical profiles of the soil behaviour type index, I_c (Robertson, 1990), versus elevation above sea level for the CPTu tests performed at San Carlo and Mirabello are shown in Figures 21a and 21b respectively. The average profiles are similar for the two sites both in horizontal and in vertical directions. The geotechnical parameters for the different units, required to assess the ground model for the local seismic response and the liquefaction hazard evaluation (see next chapter), were inferred from the results of in situ and laboratory tests carried out on undisturbed samples of fine-grained soils extracted from boreholes and disturbed samples of sandy soils from sand boils developed during liquefaction or extracted from boreholes. In Figure 22 the representative points of the fine grained soil samples are represented in the plasticity chart. They belong to lithologic units C and D. Figure 23 shows the Atterberg limits and the natural water content of the same samples versus the extraction depth. From Figures 22 and 23 can be noticed that: the sample M1-C2, taken from a depth of 12.3 m in a borehole at Mirabello, exhibited very high plasticity (plasticity index I_P = 84%, unit weight γ = 14.4 kN/m^3) and can be considered representative of organic material rather widespread in the unit C; the samples S10-C1 and M1-C3, taken from a depth of 13.3 m at San Carlo and from a depth of 17.8 m at Mirabello respectively, consist of high plasticity clayey soils (CH) with organic material content; the others samples are inorganic clays (CL).
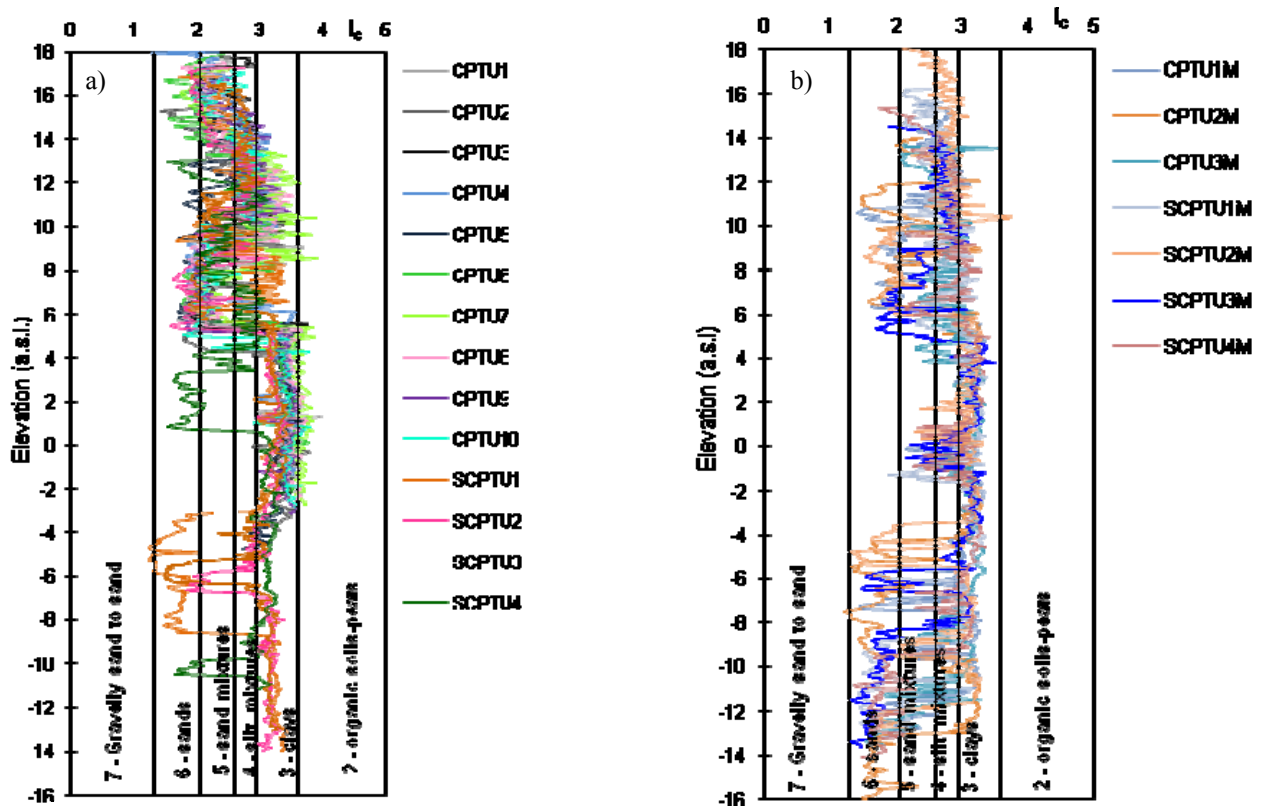

Figure 21. Soil behaviour type index, Ic (Robertson, 1990) from CPTu tests at San Carlo (a) and Mirabello (b) sites versus elevation above sea level.
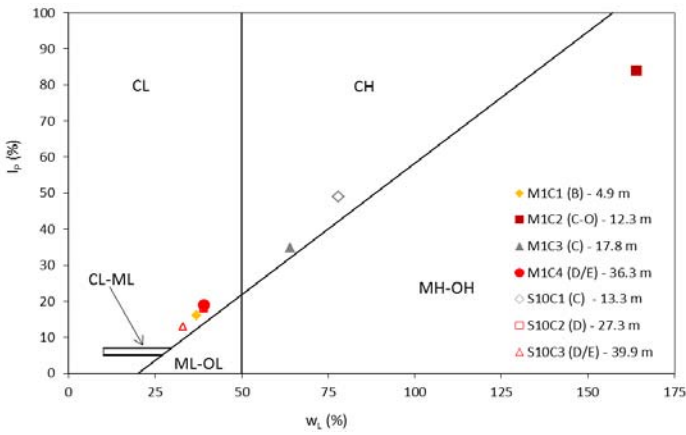
Figure 22. Plasticity chart of fine-grained and organic soils from San Carlo and Mirabello sites.

(a)

(b)

Figure 24. Experimental values of normalized shear modulus G/G_0 (a) and the damping ratio D (b) versus shear strain observed in resonant column tests on fine-grained and organic soils from San Carlo and Mirabello sites.
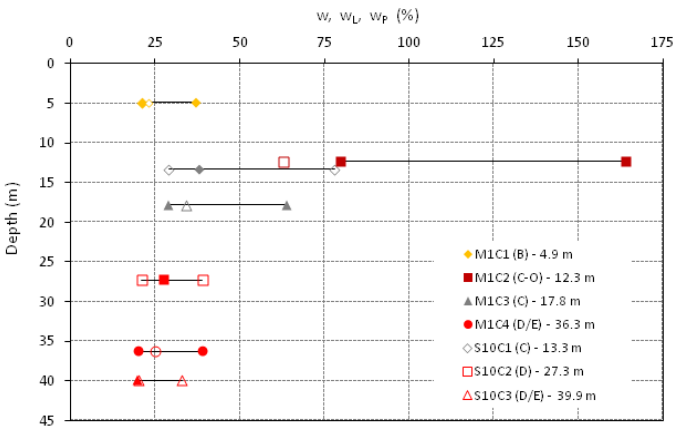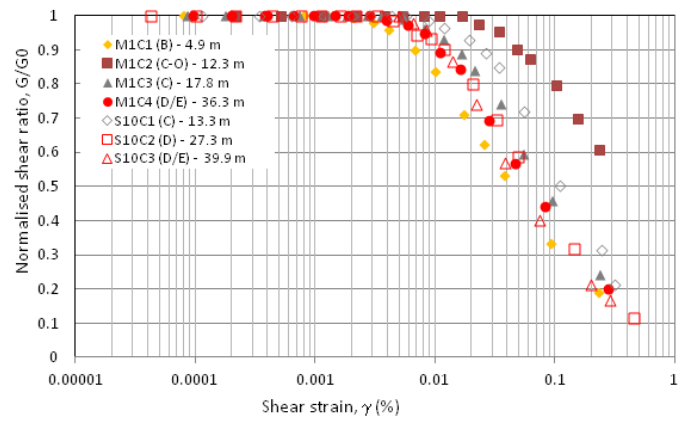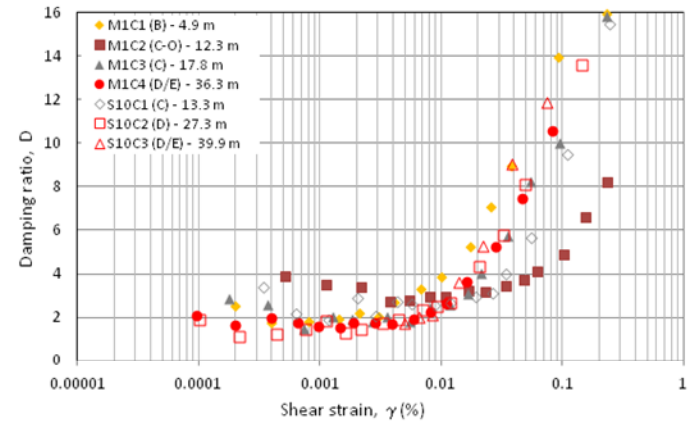

Figure 23. Atterberg limits and water content versus depth of fine-grained and organic soils from San Carlo and Mirabello sites.

Figure 24 shows the curves of normalized shear modulus G/G_0 and damping ratio D versus shear strain, obtained from resonant column test performed on the various lithological units. It can noticed the influence of soil plasticity on the shape of these curves: in particular, the curves of M1-C2 and S10-C1 samples, more plastic, degrade more slowly with shear strain than all the others. The curve of M1-C1 sample (unit B), more sandy, is located to the left of all the others; the curves of the remaining 4 samples (taken from units C and E) containing a fine fraction of lower plasticity, are similar to each other and are located in an intermediate position with respect to the other curves. The profiles of shear wave velocity, V_s, versus the elevation above sea level, from DH tests performed at San Carlo and Mirabello sites are shown in Figure 25 together with the resulting average profile. The subsoil classification according to the Italian seismic code (NTC-08) for each V_s profile are also indicated in the legend. The curves are in good agreement with each other and show very low values of V_s (not more than 200 m/s) up to an elevation of about -2 m (i.e. for the more shallow units A, B and C). At this depth the Vs profile exhibits a small discontinuity (about 100 m/s)

corresponding roughly to the transition from Holocene to Pleistocene deposits. Average V_S profiles and dispersion are similar at San Carlo and Mirabello sites from ground level to an elevation of about -16m a.s.l. At greater depths, V_S values at San Carlo are lower than those measured at Mirabello, although these depths have been reached only in a single DH test. Therefore the reference shear wave velocity profile to be assumed in ground response analysis was derived from all the DH results obtained at San Carlo and Mirabello from ground level up to -16m a.s.l., while at greater depths, where Vs trend at the two sites is different, reference was made to the profile observed at San Carlo.

Site Response Analysis
Physical and mechanical soil properties for one-dimensional ground response analysis were derived from the results of down-hole and seismic cone tests carried out at San Carlo and Mirabello from ground level to 40 m depth. At greater depths, up to the top of seismic bedrock assumed at a depth of about 120 m from ground level, reference was made to a study by Pergalani et al. (2012) concerning the seismic hazard of the Po River embankments located in the nearby Bondeno village.
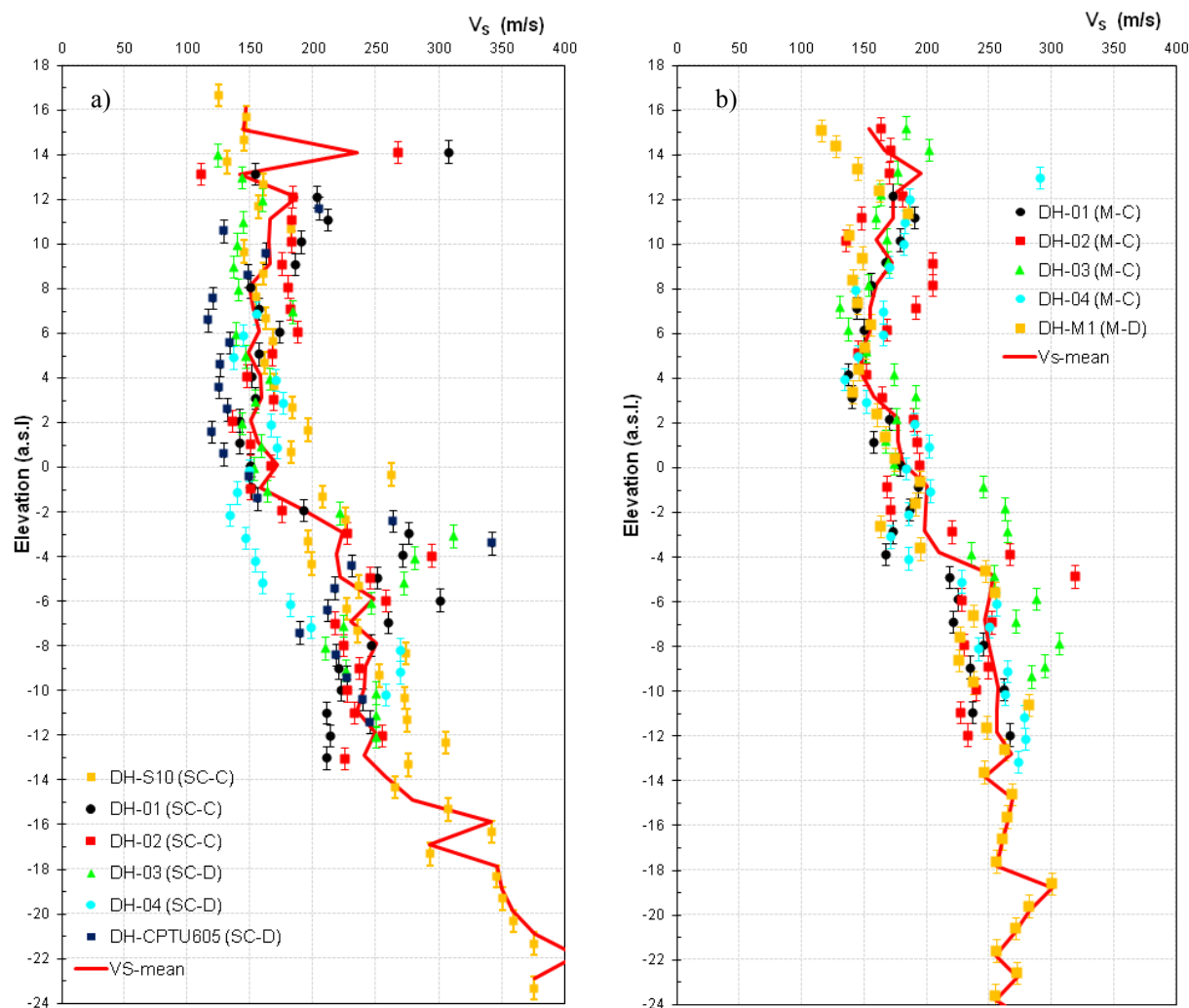
Figure 25. Experimental shear wave velocity values versus elevation above sea level from SCPTU and DH tests and average profiles at San Carlo, SC (a) and Mirabello, M (b) sites.
Subsoil class according to the Italian seismic code (NTC-08) is also indicated in brackets.

In order to investigate the influence of the embankment presence, two different conditions were considered, respectively referred to the top (A) and to the base (B) of the embankment. Stratigraphic model and properties used in ground response analysis are summarized in Figure 26 where the identifying labels of the shear modulus reduction and damping ratio curves assumed in the numerical analyses for each lithologic unit are also shown. Different curves from literature are indicated by means of the EC (Empirical Curve) symbols as follows. EC1: Seed et al., 1986 - lower bound; EC2: Seed et al., 1986 - average; EC3: Sun et al., 1988 - Clay (IP = 40-80%); EC4: Idriss and Sun, 1992. The others symbols refer to experimental curves from resonant column tests carried out on a number of samples from San Carlo and Mirabello sites. Reference peak ground acceleration and seismic input motions adopted in ground response analyses (I1, I2 and I3) were selected according to the Emilia-Romagna regional guidelines for the seismic microzonation (D.A.L., 2007). Acceleration time histories of the three input motions are shown in Figure 27.

Figure 28 shows ground response results in terms of pseudo-acceleration response spectra (5% of critical damping) compared with the corresponding spectra of the seismic input signals. For the two vertical soil profiles analyzed, the parameters of input and output seismic signals are summarized in Table 3 together with the amplification factors expressed in terms of PGA and Housner Intensity. It can be observed that the seismic response is very similar for the two vertical profiles and the value of the average amplification factor in terms of PGA $(FA(PGA)_{av} = 1.40)$ is close to the value obtained from Pergalani et al. (2012) at the Bondeno area $(FA(PGA) = 1.44)$ as well as to the one deduced from the Italian seismic code (NTC-08) for subsoil Class C (FA(PGA) = 1.47) in which most of the sites examined falls.

Site amplification effects on the damage of the Mirandola bell-tower
The masonry bell-tower of the Mirandola cathedral is about 45 m tall. The structural damage observed after the seismic events was accurately reported by Pesci & Bonali (2012) using laser-scanner survey.
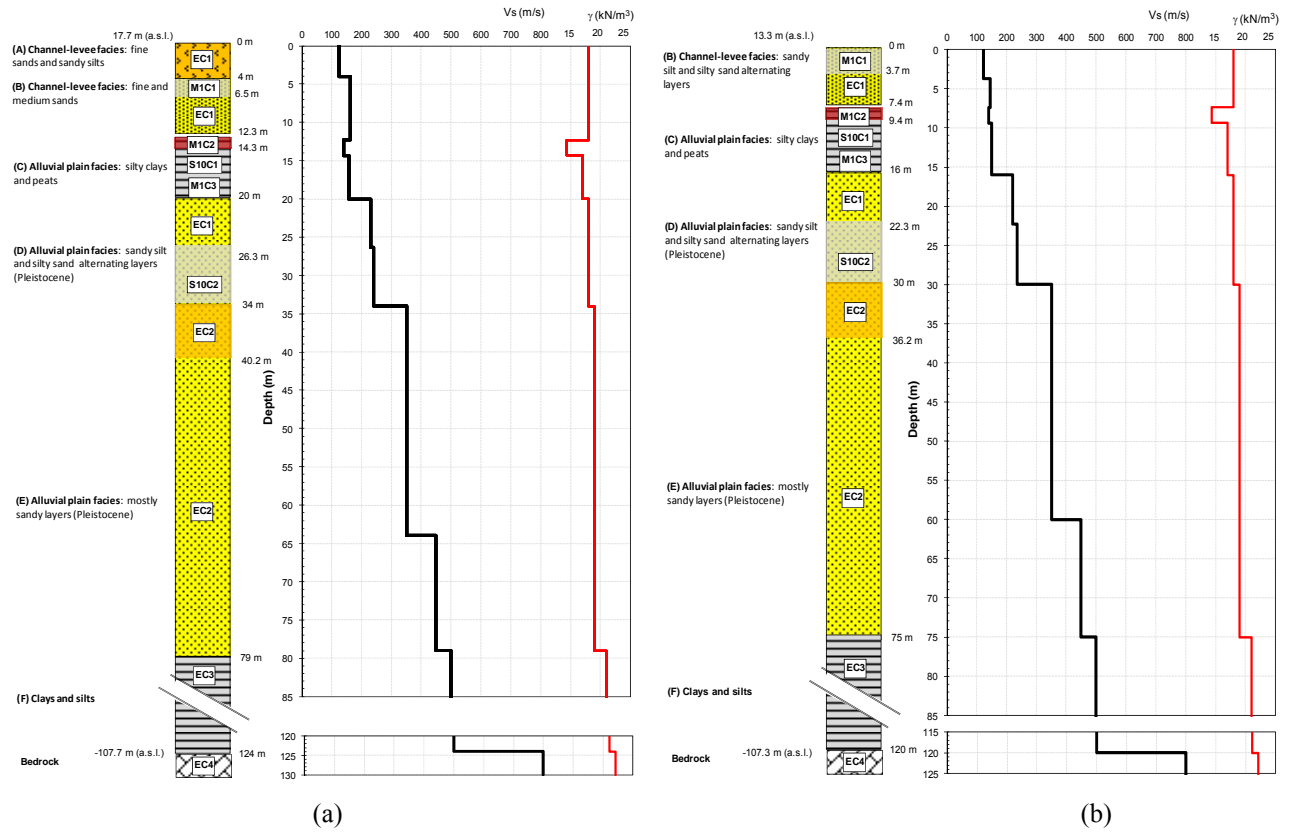
Figure 26. Lithologic units, shear wave velocity and soil unit weight profiles assumed for ground response analysis at the vertical soil profile: a) A (top of the embankment); b) B (base of the embankment).
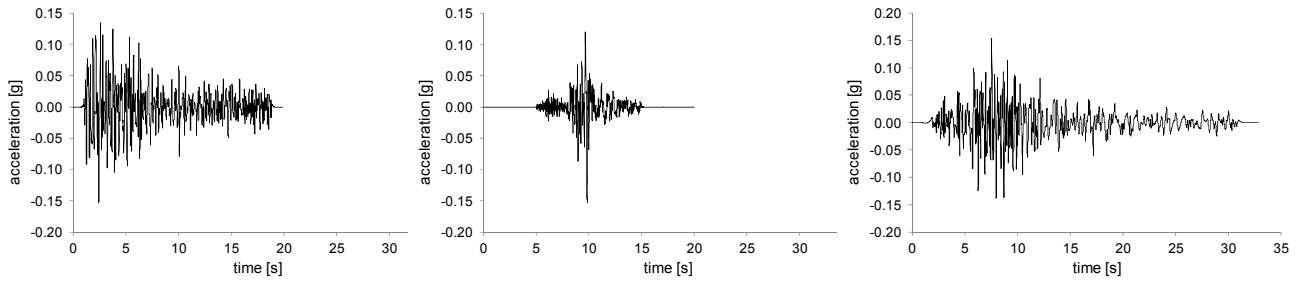
Figure 27. Acceleration time histories of the input motions (the main parameters are summarized in Table 3).

Table 3 - Main parameters (PGA: peak ground acceleration; I_a: Arias Intensity; T_0: fundamental period; D_T: Trifunac duration) of seismic inputs (I1, I2 and I3) and outputs (O1, O2 and O3) from ground response analysis at vertical soil profile A (top of the embankment) and B (base of the embankment) and corresponding amplification factors, FA(PGA) and FA(I_H) in terms of PGA and Housner Intensity respectively.

	I1	I2	I3	O1-A	O2-A	O3-A	O1-B	O2-B	O3-B
PGA (g)	0.153	0.153	0.153	0.218	0.228	0.191	0.238	0.222	0.175
I_a(cm/s)	0.26	0.07	0.29	0.46	0.17	0.81	0.41	0.17	0.80
T_0 (s)	0.4016	0.4357	0.7585	0.402	0.975	0.758	0.402	0.975	0.758
D_T (s)	8.85	1.205	12.89	14.56	2.56	17.32	13.52	3.195	21.07
FA(PGA)				1.42	1.49	1.25	1.56	1.45	1.14
FA(I_H)				2.31	2.49	2.76	2.41	2.58	2.71
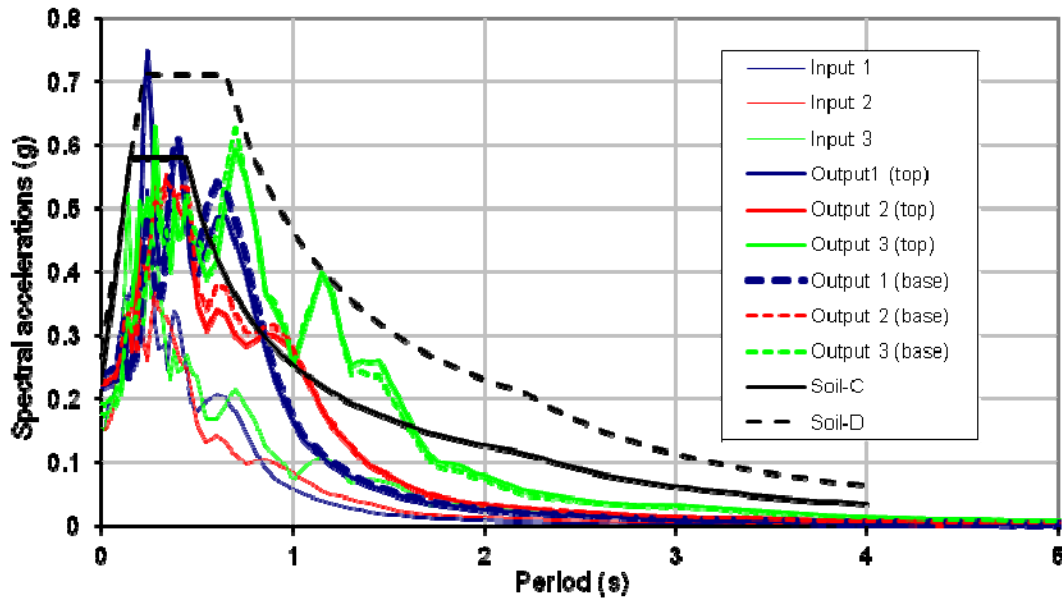
Figure 28. Pseudo-acceleration response spectra (5% of critical damping) of the seismic input motions and output signals at the vertical soil profile A (top of the embankment) and B (base of the embankment) compared with the spectra suggested from the Italian seismic code (NTC-08) for subsoil classes C and D.

In particular, Pesci & Bonali (2012) noted that the intermediate part of the tower, between 20 m and 32 m height, had twisted (in torsion) with a maximum relative displacement of about 10 cm (i.e. a rotation of about 1°) with respect to the underlying part of structure. The observation of parallel linear cracks (Fig. 29), keystone failure and plastic hinges confirm the torsional mechanism of the upper part of the tower.

T_1 and T_2 are the fundamental periods of the first two bending modes along the horizontal directions x and y (where x corresponds to the lower flexural stiffness of the tower), T_3 is the first torsional vibration mode, and T_4 is the period of the second bending mode along x direction.
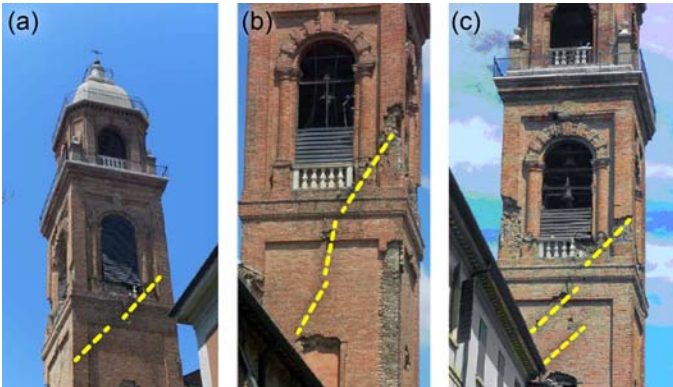
Fig. 29. Damage of bell-tower of the Mirandola cathedral (a) east view, (b) west view and (c) south view (adapted from Pesci & Bonali 2012).

The reasons for such a particular damage mechanism could be sought through a simplified analysis of the dynamic response of the tower with reference to the ground motion recorded at the nearby seismic station MRN. In the case of masonry towers, the fundamental frequencies of vibration of the structure mainly depend on the dimensions of structural elements, i.e. aspect ratio and slenderness, the material properties and also other factors like connections to adjacent buildings, and so on. The typical shapes of the first four vibration modes for a tower are shown in Fig. 30. The periods
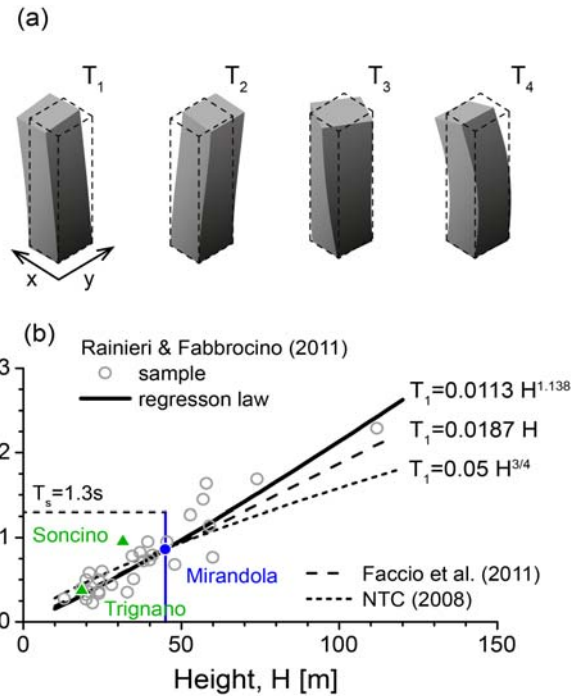
Figure 30. (a) Schematic shapes of the vibration modes of a tower with higher stiffness along y axis; (b) computation of 1st resonant period of Mirandola bell-tower and other case studies (Rainieri & Fabbrocino, 2011).

In this preliminary analysis, the modal periods of tower could be estimated using simplified empirical relationships suggested by Rainieri & Fabbrocino (2011). These were obtained from a dataset of predominant period values evaluated from the dynamic response of 30 Italian masonry towers (mainly in Molise region), which were either monitored measuring the environmental vibrations, and/or analysed numerically. The same authors suggest to estimate the first fundamental period, T_1, as a power function of the tower height, H, only, while the higher mode periods can be expressed as proportional to T_1 by means of suitable reduction coefficients (see Fig. 31). In the Fig. 31, the value of T_1 computed with the relationship of Rainieri & Fabbrocino (2011) is compared with those predicted by the power function recommended by the Italian Technical Code (NTC, 2008). It is singular to note that, for this particular value of the tower height, all the empirical relationships considered yield the same value of $T_1 = 0.85s$. In the same figure, a dashed line also indicates the fundamental subsoil period, $T_s = 1.3$ s, of the MRN seismic station, that is located about 450m from the tower, on a deep Quaternary soft deposit, where the seismic bedrock can be located as deep as 125 m (WG-DPC, 2012). In the Fig. 31 the estimated values of the first four mode periods are compared with the pseudo-acceleration response spectra, S_a, of the horizontal components recorded at Mirandola station (red lines). The comparison highlights that the predominant period of WE ground motion component is comparable to the first torsional mode of the tower, T_3, confirming the observed damage mechanism. At the same time, the predominant period of the NS component is close to the resonant period, T_4, of the second bending mode along x direction. It can be therefore hypothesized that the damage observed on the bell-tower may be the result of the superposition of both torsional and secondary flexural mechanisms.

LIQUEFACTION

Liquefaction evidences and damage

Significant and widespread liquefaction effects, which caused panic of inhabitants and damage to buildings and infrastructures, were observed in various areas of Emilia-Romagna region, during the seismic events of May 2012. These phenomena have mainly involved the old river bed deposits and the ancient levees of the Reno River, principally at the two villages of San Carlo (Municipality of Sant'Agostino) and Mirabello. Phenomena of minor entity and diffusion were observed also in other sites (eg. Dodici Morelli, San Felice sul Panaro, etc.), but always in similar geo-morphological conditions (Figure 32).

San Carlo and Mirabello, where major liquefaction impacts were produced during May 20 ground shaking, are typically small industrial and farm inhabited centers of Po Valley with masonry or concrete two or three-story buildings with shallow foundations. In Figures 33 and 34, the main observed liquefaction effects at San Carlo and Mirabello are sketched.

On 20th May, the main shock of magnitude 5.9 produced strong ground motions, especially in the vertical direction. Liquefied sand erupted and flooded many large areas of the two villages. As Figures 35 and 36 show, the surface phenomena observed immediately after the quake were typical soil liquefaction evidences, that is: sand boils, vents, sinkholes, craters, surface ruptures, extensional fissures. Many open spaces, as courtyards, gardens and roads, were completely covered by the ejected sand, mud and water. The thickness of erupted material was in many cases more than 30 cm. In some buildings, from pavement cracks the sand uplifted even for about 100 cm.
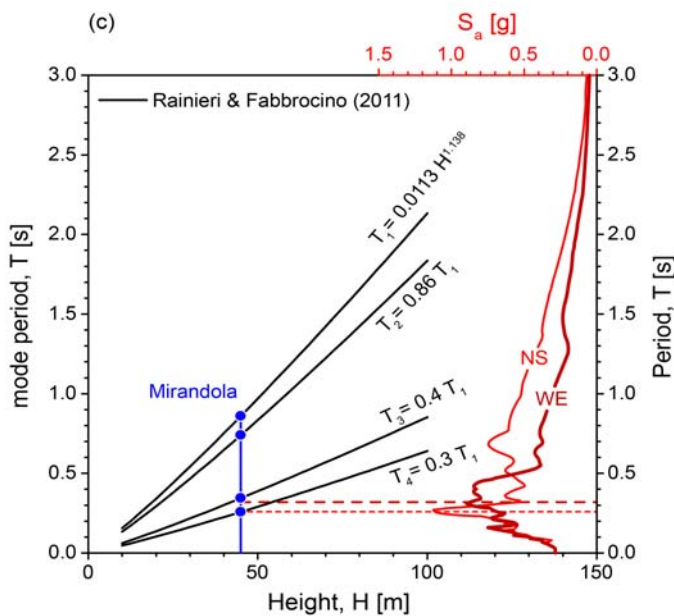

Figure 31. Comparison between the estimated four resonant periods and the response spectra of the main-shock of the seismic sequence recorded at Mirandola station.
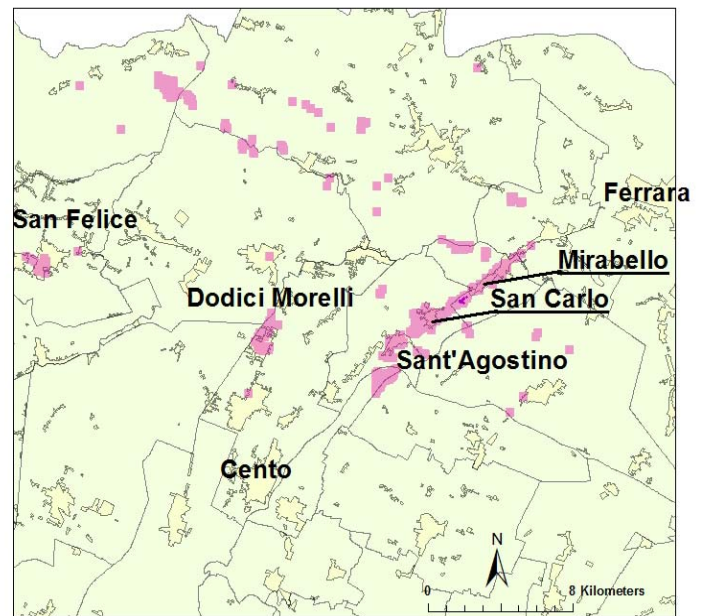

Figure 32. Map of soil liquefaction phenomena observed during the Emilia-Romagna earthquakes of May 20 and 29, 2012.

Figure 33. Map of observed liquefaction effects at San Carlo village (continuous lines: soil ruptures; cross: sand boils and volcanoes, vents, flooding from swells,...; hatched rectangles: foundation settlements and rotation). Dashed lines delimit pale-channels area.

Figure 34. Map of observed liquefaction effects at Mirabello village (continuous lines: soil ruptures; cross: sand boils and volcanoes, vents, flooding from swells,...; hatched rectangles: foundation settlements and rotation). Dashed lines delimit paleo-channels area.

The erupted sands appeared fine graded, relatively clean and of uniform size. Some gas and water pipelines were broken. Many roads were fissured. Residents described high water spouts issuing from the fissures following the earthquake.

Nevertheless, the severity of liquefaction damage was different in the various zones and varied even within one zone passing from severe to low.

Even if the impacts were spectacular in some sites and absolutely unusual in the Italian context, neither relevant ground settlements nor considerable lateral spreads nor extended flow liquefaction phenomena were observed. There was also clear evidence that ground settlements were in general relatively uniform and limited. Moreover, the foundation systems of the buildings supported generally well the overlain structures. Tilting and overturning of foundations occurred cannot explain the collapsed industrial plant buildings; the collapse seemed to be imputable more to the structural vulnerability than to the liquefaction even if the occurrence of liquefaction might play some role.

More important and widespread damages resulted for buried lifelines (gas and water pipelines).

A few cases of re-liquefaction at San Carlo and Mirabello, even not so intensely than during the sequence of May 20, were reported following the event of May 29. Unfortunately, no certain documentation exists for this second occurrence as the two villages were partially evacuated. With regard to the earthquake on 29th May, it must also be noted that the hypocenter was deeper than those of the 20th May sequence and the epicentral distances of San Carlo and Mirabello were larger.

Instead, some sites closest to the epicenter (for instance San Felice sul Panaro) where minor liquefaction effects were observed on May 20, re-liquefied more intensively as a consequence of the May 29 event, but with negligible effects on ground and structure stability or lifeline serviceability.

Subsoil conditions and liquefaction susceptibility
The subsoil conditions in the areas of San Carlo and Mirabello are widely described in previous sections. In particular with regard to liquefaction susceptibility it is worth noting that the water table level of May 2012 just before the seismic events was in its seasonal peak (about 80-130 cm from ground surface). After the main events, a considerable number of surveys was performed in the area struck by the Emilia-Romagna seismic sequence on May 2012 to accurately test the liquefaction susceptibility of the soil deposits affected by the most severe liquefaction-induced effects and damages. The assessment is based on a review of more than 20 sites located at San Carlo and Mirabello where sand boils, ground failures, horizontal ground displacements and foundation settlements occurred. In situ and laboratory test results were collected from 8 seismic piezocone penetration tests (SCPTu), 2 down-hole tests (DH), 21 piezocone penetration tests (CPTu), 28 boreholes (BH) and a number of size-grain distribution and consistency limit tests performed on the extracted samples. A typical subsoil vertical profile at San Carlo (Figure 37), deduced from the borehole 185130P432 (Figure 33) of Regional database, consists of a shallow silty layer (2 m thick) overlying medium to fine sands (5 m thick) underlying by a thick layer of clay. Beneath that, at a depth of about 19 m, a 4 m thick layer of coarse to medium sand was encountered.
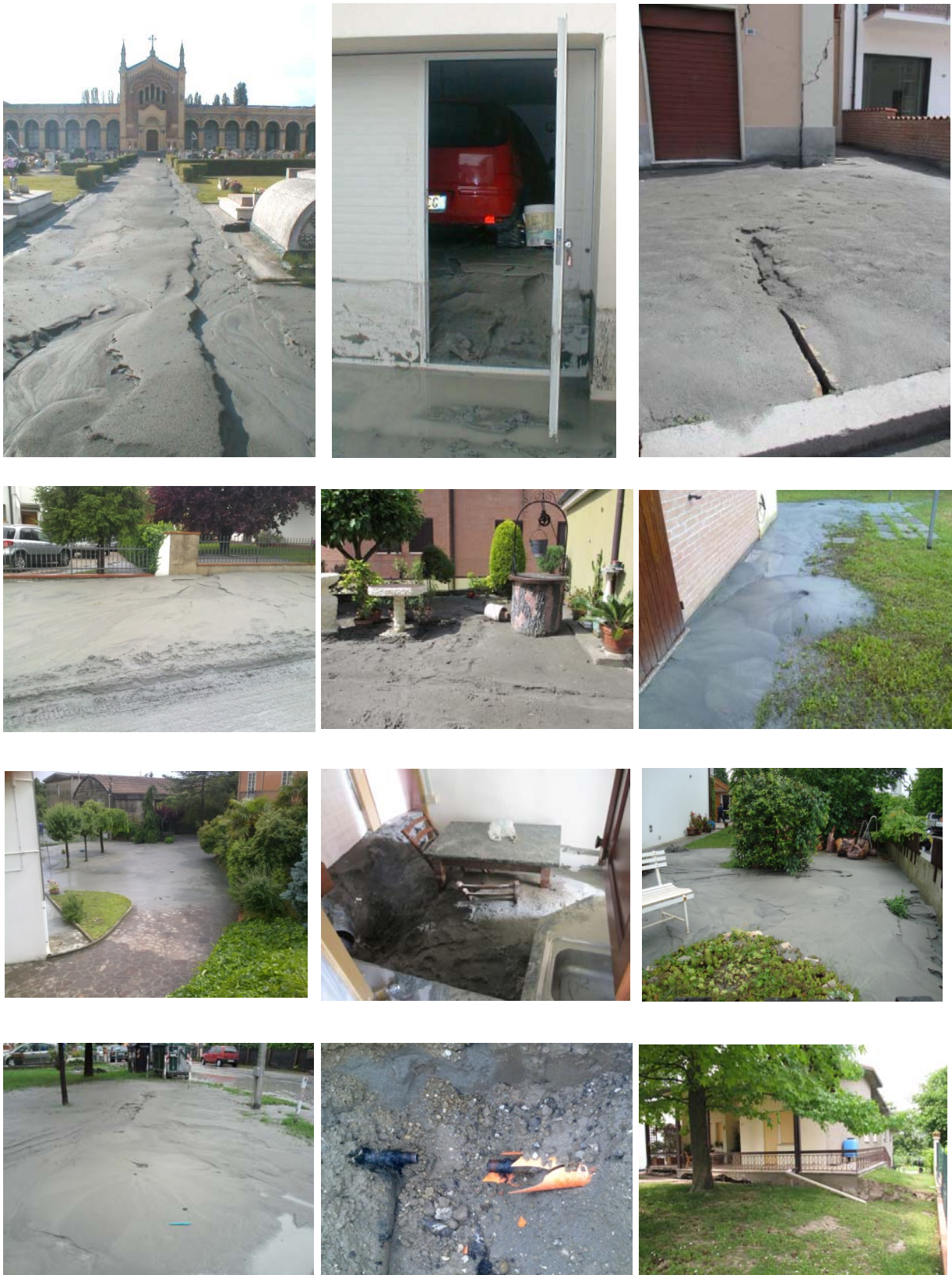
Figure 35. Liquefaction evidences and damages at San Carlo (photos by DICeA Geotechnical team)

Figure 36. Liquefaction evidences and damages at Mirabello (photos by DICeA Geotechnical team)

A deep trench (Figure 38) has been excavated at San Carlo after the shocks of May 20. It revealed the presence of superficial non liquefiable soils overlying the liquefiable layer and clear sub-vertical paths of the liquefied sand that reached the surface, causing, in free field conditions, sand boils, volcanoes, large and long cracks. Grain size distribution curves of several samples of liquefied ejected sands (Figure 39) compared with critical curves suggested by the Italian seismic code (NTC-08) indicates material susceptible of liquefaction.
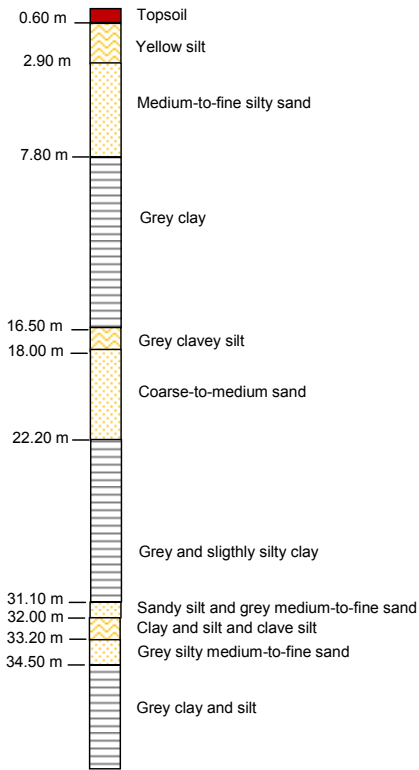
Figure 37. Soil profile at San Carlo from BH 185130P432 of Regional database.

Soil profile labels:
- 0.60 m — Topsoil
- 2.90 m — Yellow silt
- Medium-to-fine silty sand
- 7.80 m — Grey clay
- 16.50 m — Grey clavey silt
- 18.00 m — Coarse-to-medium sand
- 22.20 m — Grey and sligthly silty clay
- 31.10 m — Sandy silt and grey medium-to-fine sand
- 32.00 m — Clay and silt and clave silt
- 33.20 m — Grey silty medium-to-fine sand
- 34.50 m — Grey clay and silt

Analysis of the liquefaction hazard

The liquefaction hazard was estimated for each CPTu profile (see Figure 21) using the simplified procedure of Robertson and Wride (1998) modified according to the Youd et al. (2001) suggestions. Simplified procedures are based on the "cyclic stress approach" and allow the liquefaction potential of each investigated layer be expressed in terms of safety factor (deterministic approach) or probability (probabilistic approach) or another index obtained from the comparison
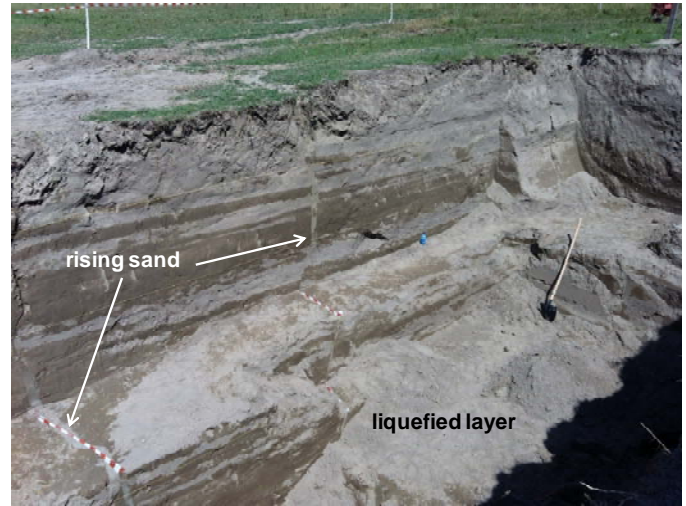

Figure 38. Deep trench (6m depth) at San Carlo (photos by DICeA Geotechnical team).

Legend:
- SAN CARLO Via 8 marzo (S)
- SAN CARLO Via Verga (S)
- SAN CARLO S1 (BH-9.5 m)
- SAN CARLO S3 (S)
- SAN CARLO S3 (BH-5.5 m)
- SAN CARLO S3 (BH-9.5 m)
- SAN CARLO S3 (BH-11.5 m)
- SAN CARLO S4 (S)
- SAN CARLO S4 (BH-4.5 m)
- SAN CARLO S4 (BH-7.3 m)
- MIRABELLO Corso Italia (S)
- MIRABELLO Via dell'argine vecchio (S)
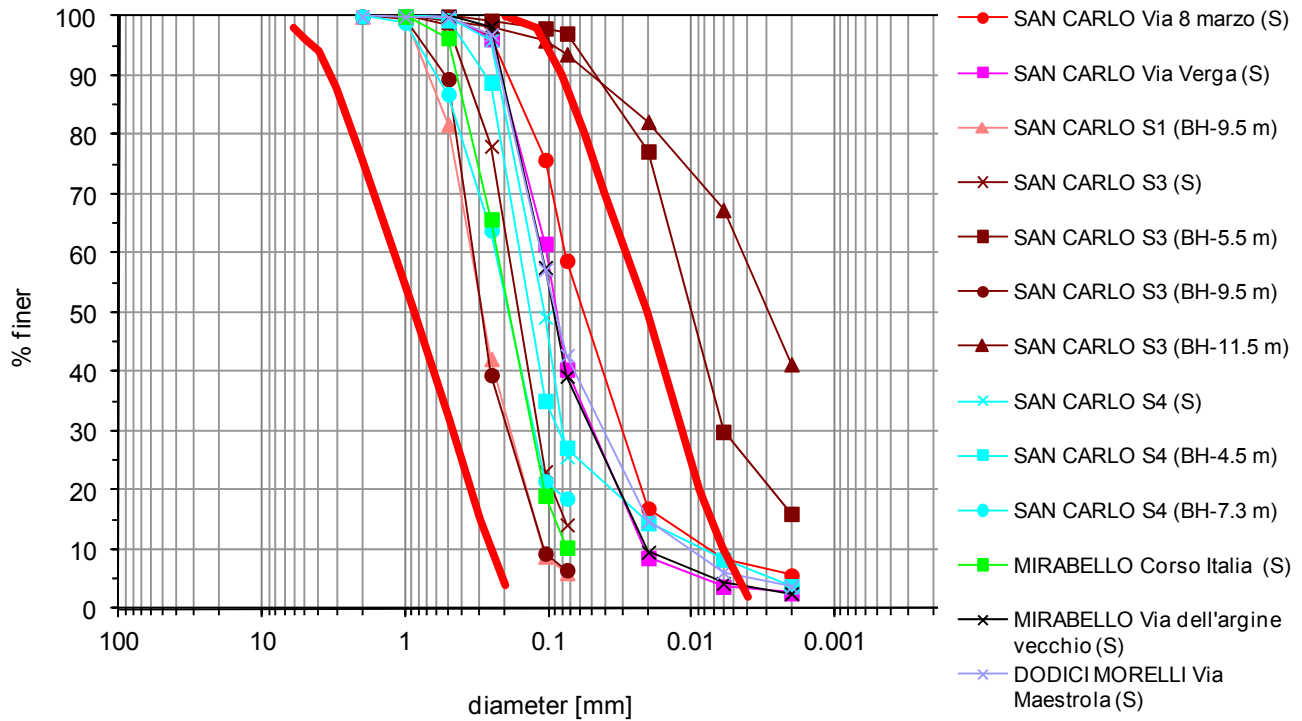- DODICI MORELLI Via Maestrola (S)

Figure 39. Size-grain distribution of undisturbed samples from boreholes S1, S3 and S4 (San Carlo) and samples of liquefied ejected sands compared with critical curves suggested by the Italian seismic code (NTC-08).

between the earthquake induced loading and the liquefaction resistance of soil, both expressed in terms of cyclic shear ratio (CSR and CRR, respectively). Semi-empirical relationships are generally used to estimate CSR and CRR; many of them have been collected and critically reviewed by Youd et al. (2001) and Seed et al. (2003). A cumulative index of liquefaction potential (LPI) of the liquefiable layers in the first 20 m of depth, originally introduced by Iwasaki et al. (1978), is finally calculated to provide a single value of liquefaction potential of each investigated vertical profile and to assign the corresponding hazard level. Simplified procedures only implement a 1-D (free-field) model with horizontal S-wave propagating (horizontal ground accelerations); the effect of P-waves (and vertical ground accelerations), the geometry of liquefiable layers, the presence of static shear stresses (driving stresses) are generally neglected as well as they do not directly include a specific pore water pressure buildup law or a degradation law for soil resistance. The following data were used in the liquefaction analyses performed by means of the aforementioned procedure: water table depth located between 0.8 and 1.3 m from ground level, design ground acceleration on ground type A, a_g = 0.153 g at San Carlo site, and a_g = 0.145 g at Mirabello site according to the Italian Seismic Code (NTC-08), stratigraphic amplification factor S_S = 1.5, expected magnitude M_w = 6.14, corresponding to the value for the seismogenetic zone 912 as suggested by the Italian guidelines

on the Seismic Microzonation (DPC, 2008), Magnitude Scale Factor MSF = 1.8, as suggested by the EC8 (2003) and by Youd et al. (2001). Figure 40 shows the results obtained for each analyzed vertical profile in terms of Liquefaction Potential Index (LPI) versus elevation above sea level.

On the basis of the LPI values, the maps of liquefaction hazard (Figure 41), depth from ground level of the top of the liquefiable layer (Figure 42) and thickness of the liquefiable layer (Figure 43), both at San Carlo and Mirabello sites, were finally assessed using the natural neighbour interpolation technique (Sibson, 1981).

The analysis results in terms of Liquefaction Potential Index (LPI) shown in Figure 40 do not seem to fully explain the great diffusion and extension of the liquefaction effects observed at San Carlo and Mirabello during the ground shaking of May 20.

It is well known that liquefaction is a complex phenomenon dependent on various factors: triggering factors (earthquake characteristics: magnitude, amplitude of acceleration, duration, etc.) and susceptibility factors (soil properties, water table depth, morphology, presence of buildings, shear stress conditions before ground shaking, etc.).

The observed scenario of effects produced by the Emilia-Romagna earthquake on May 20, 2012 shows that several factors have contributed to increase the seismic demand and to reduce the availability of soil liquefaction resistance.
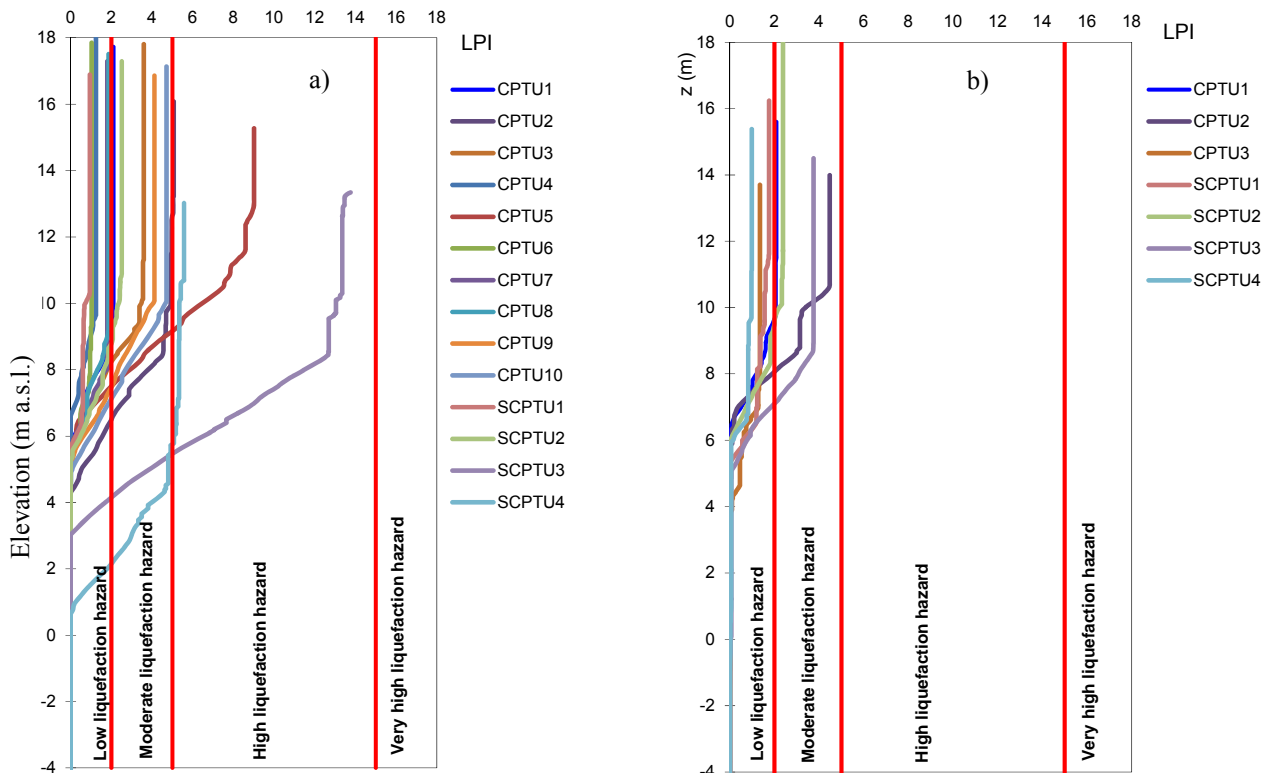

Figure 40. Liquefaction Potential Index, LPI (Iwasaki et al., 1978) from CPTu tests at San Carlo (a) and Mirabello (b) versus elevation on the sea level.
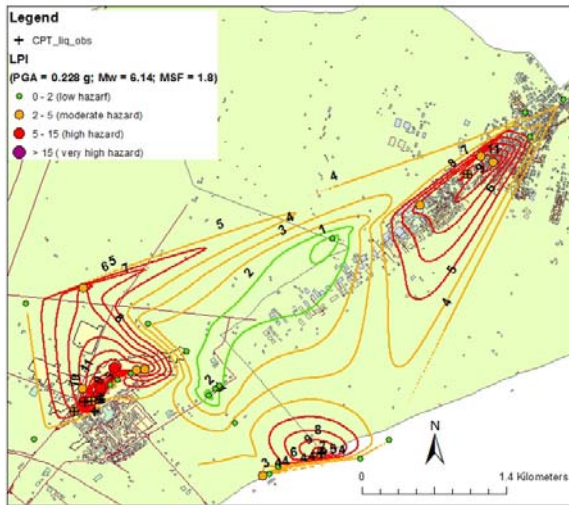
Figure 41. Liquefaction hazard map from simplified procedure based on CPTu tests at the San Carlo and Mirabello area.
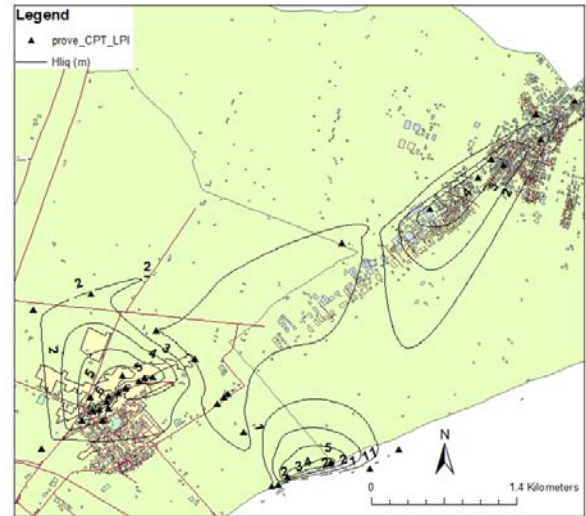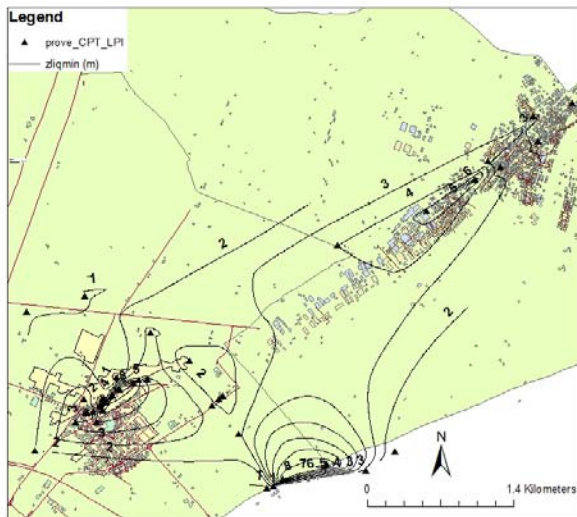

Figure 42. Map of the depth from ground level of the top of the liquefiable layer from simplified procedure based on CPTu tests at the San Carlo and Mirabello area.

As concerns the demand, key factors were the shallow hypocentral depth (6.3 km) and the short epicentral distances (less than 20 km). Probably this also led very high peak ground acceleration of the vertical components. As a matter of fact no recordings are available at San Carlo and Mirabello sites, but at Mirandola recording station, located about 13 km from the epicenter, the peak ground acceleration of the vertical component (0.309g) was larger than those of both the horizontal components (0.264g and 0.261g). Moreover, since triggering of liquefaction is also related to the number of significant load cycles, another important factor might have been the rapid succession in three and half minutes of two shocks of magnitude 5.9 and 5.1. It is plausible that the impacts might have been the sum of those of two earthquakes. The influence of this factor is going to be analyzed through numerical simulations when higher-quality geotechnical data will be available.

Figure 43. Map of the thickness of the liquefiable layer from simplified procedure based on CPTu tests at the San Carlo and Mirabello area.

As concerns the soil liquefaction resistance, its rapid reduction during the earthquake could be ascribed to the following factors: recent age of superficial deposits in reclamation zones (paleoalveos and embankments), soil composition (sands and silty with a clay fraction < 10%), in situ state (very loose in the upper strata), water table close to the ground surface. Confining pressure had a leading role in reducing the loss of soil resistance as evidenced by the liquefaction phenomena experienced by the foundation soil of buildings smaller than those observed in free field conditions.

The wealth of data already available permits that the following conclusions be drawn. The liquefaction manifestations induced by the earthquake of May 20, 2012 at San Carlo and Mirabello in free field, can be classified from moderate to severe; while the impacts on ordinary buildings were not so severe. Even if the volume of ejected sand was in many case impressive, soil deformations below the building were almost less than the values suggested by Youd (1998) as indicative of high liquefaction risk, that is 30 cm for lateral displacements and 10 cm for vertical settlements. In our case, it must be underlined that the vertical displacement, in some case up to 40 cm, was much greater that the horizontal one, almost not significant. The satisfactory behaviour of some ordinary buildings could be attributed to the performance of the shallow foundations with perimeter footings connected by grade beams. Damage from moderate to severe was observed in gas and water lifelines and roads.

The liquefaction hazard, estimated by using the Robertson and Wride method applied to the CPTu tests carried out in the area after the earthquake and expressed by the Liquefaction Potential Index (LPI), appears moderate. This result is in contrast with the soil liquefaction effects observed during the seismic event of 20th May. Therefore, the simplified methods for estimating the liquefaction hazard seem to require a refinement in order to obtain quantitatively reliable results for regional seismic conditions.

INDUSTRIAL BUILDING FOUNDATION BEHAVIOUR

Industrial building foundation: damage and current typologies of foundations

Many industrial buildings collapsed or suffered great damage during the 20-29 May 2012 Emilia-Romagna seismic events. This caused enormous problems to the industrial activity, which is among the most profitable of Italy in the region.

Damage observed on industrial buildings are due to structural and geotechnical shortcomings. All these shortcomings are mainly due to the late seismic classification of this area; so the majority of existing industrial buildings have been designed without anti-seismic criteria. The structural engineer scientific community has recently published guidelines regarding the main structural shortcomings of industrial buildings and their seismic upgrading (WG-RELUIS, 2012).

Geotechnical shortcomings are due to foundation typologies not suitable to withstand seismic actions, fractures occurred in the soil, as well as soil liquefaction.

Figure 43 shows the effect of soil liquefaction in an inspected industrial building: soil liquefaction produced in the industrial pavement fractures, through which the soil is spilled. Figure 44 shows the damage occurred on a column of the same inspected building of Figure 43, which could be due to the seismic action on the column, as well as to the foundation rotation caused by the liquefaction on by the lack of bearing capacity of foundation in seismic conditions.

An extensive description of liquefaction phenomena occurred during the 20-29 May 2012 Emilia-Romagna seismic events is reported in this paper in the liquefaction section. In the following damage due to foundation shortcomings, existing foundation typologies, as well as design criteria for foundation seismic upgrading will be discussed. A more extensive description on geotechnical shortcomings of Emilia-Romagna industrial building foundations are reported in the recent guidelines by WG-AGI (2012).

Many of the observed damage related to foundation behavior can be associated to footing rotation, to fractures occurred in the soil, a part from soil liquefaction. In some rare case the hammering produced by the industrial pavement on the columns, not opportunely jointed to the pavement, causes significant damage.

Figure. 43. Damage on an industrial building due to soil liquefaction

Figure 45 shows the evident rotation of a column of an industrial building. This column rotation was very probably due to the corresponding footing rotation. Connections opportunely taken into consideration in the design of the whole industrial building including foundation, probably would have avoided the observed damage.

Figure 46 shows significant fractures on the wall of an inspected industrial building due to soil fractures.

Figure. 44. Damage on an industrial building due to hammering on a column by the rigid industrial pavement.

Figure 45. Damage on an industrial building due to foundation rotation.

Figure 46. Damage on an industrial building due to fractures in the soil.

The majority of industrial buildings of the examined area are characterized by one elevation and one span. They were constructed before the 2003 "Seismic classification of Emilia-Romagna"; thus they are characterized by isolated shallow footings (Figure 47).

In same rare cases, due to soil properties, footings with pile, having generally a length L = 15-20 m and a diameter D   60 cm, were made (Figure 48). After 2003 footings have been designed following seismic criteria; thus, first of all crossed-connection elements between footings have been included.

In any case immediately above the footings an industrial pavement is present, this pavement has a thickness of about 15-20 cm and is reinforced with a wire netting (Figure 49).

The industrial pavement presents construction joints, expansion joints and joints to the cast phases. Across these last kind of joints steel rods are used. Expansion joints do not involve whole the pavement thickness. It is important to underline that around the columns expansions joints were commonly designed, but very often not realised.

Generally foundations of existing industrial buildings consists of prefabricated isolated sleeve-footings. Sleeve-footing plan dimensions vary from 1.30x1.30m2 to 5.0x5.0m2, the height varies from 0.60m to 1.10 m. Greater dimensions can be necessary for footings related to more than one column. Sleeve-footing are resting above a reinforced concrete sub-foundation. The sub-foundation is reinforced with a wire netting and has a thickness of 30÷40 cm (Figure 50). Only a frictional interaction exists between the sleeve footing and the sub-foundation.

Criteria for the seismic improvement of foundations
According to the Legislative Decree n. 74 of the June 6, 2012, (D.L. 6.VI.2012, No. 74., 2012) issued soon after the main seismic events, the rehabilitation measures for the seismic upgrading of industrial building footings can be subdivided into two categories:

i) measures for the rapid attainment of safety, in order to obtain the provisional Statement of Conformity,

ii) measures for the full attainment of safety, in order to obtain the final Statement of Conformity. The former consist of simple retrofit measures, carried out without any demolition works, to mitigate the principal seismic deficiencies. They do not require any official design verifications. The latter need to be implemented following the usual safety design criteria, and are more invasive, expensive and not of rapid execution; more specifically, demolitions and field operations in the foundation soils are often needed. After rehabilitation, the existing building should be characterized by a structural performance compatible with seismic demand at least equal to 60% that of a new building. Table 4 schematically summarizes the principal seismic deficiencies of the industrial building footings and the related possible rehabilitation measures.
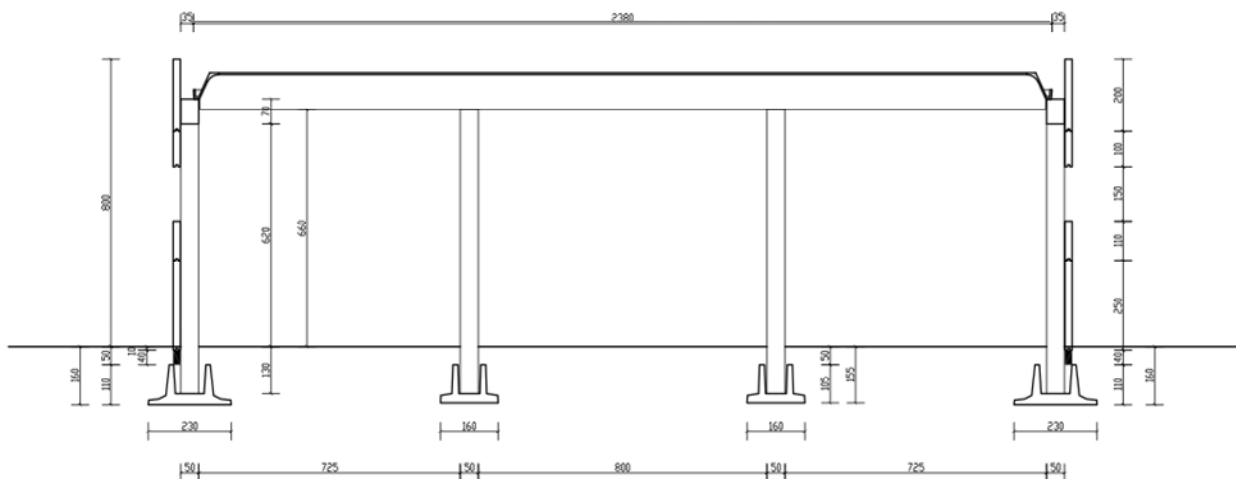

Figure 47. Section view of an existing industrial building in the examined area, with shallow foundations.

Figure 48. Section view of an existing industrial building in the examined area, with pile foundations.

Table 4. Rehabilitation measures for the seismic upgrading of industrial building footings.

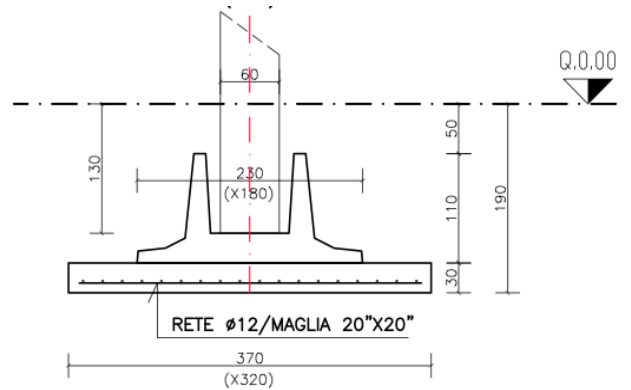| Principal seismic deficiency	Failures	Vertical differential settlements	Horizontal differential settlements	Rotations	Absolute settlements	Rehabilitation measures
Inadequate structural capacity	X					Reinforcement of the foundation structure (hoops and links between columns and footings, etc.)
Lack of cross-connection elements		X	X	X		Cross-connection elements (connecting beams, tie rods, etc.)
Inadequate bearing capacity				X	X	Enlargement of footing-plan dimensions; underpinning with micropiles or piles with medium diameters, jet grouting etc; new footings
Soil liquefaction	X	X		X	X	Soil improvement using grouting, chemical stabilization, deep mixing, drainage, etc.

In some cases it was possible to associate these deficiencies to the damage exhibited by the buildings during the recent earthquake, but in general foundation and soil conditions can hardly be documented only by external surveys.

Figure 49. View of the industrial pavement during construction.

Figure 50. Sleeve-footing on reinforce concrete sub-foundation.

Deficiencies related to the structural behaviour of footings are often associated to inadequate size of the sleeve footing neck, and to insufficient bending and shear strength of the sleeve walls. In these cases, the countermeasures can consist of the plinth reinforcement and of the strengthening of foundation-column connection.

Geotechnical deficiencies are essentially connected to the lack of cross-connection elements between the footings. In these conditions, inertial forces can induce significant differential settlements, horizontal displacements and rotations at the foundation level with consequent damage to the elevation structures. As observed during the post-earthquake inspections, the industrial pavement, frequently cast in place without any separation joints with the building columns, played probably the role of horizontal connection element, reducing the level of damage. Thus, even if the role of industrial pavement can be generally very useful, it has to be analysed carefully.

More in general, building footings can be characterized by inadequate bearing capacities due to insufficient values of soil strength and/or foundation dimensions, especially with reference to seismic actions. This situation can cause

excessive absolute settlements and rotations. The seismic retrofit can consist in the enlargement of the footing-plan dimension or in underpinning works.

Finally, important deficiencies can arise from liquefaction (see liquefaction section) phenomena of the foundation soils. Appropriate mitigation techniques, such as grouting, chemical stabilization, deep mixing and drainage, should be carefully designed not to induce significant movements in the existing buildings.

Seismic Assessment and Improvement of Industrial Building Shallow Foundations

The practice of improving the seismic performance of existing buildings (also known as seismic rehabilitation, seismic retrofitting, or seismic strengthening) began in the Unite States in the 1940s for pre-1933 school buildings. From that period, much efforts have been made to mitigate the risks from seismically deficient masonry and reinforced concrete buildings. During 2012 Emilia-Romagna Earthquake, several industrial precast structures collapsed or underwent severe damages. After the event, the ReLUIS (Laboratories University Network of Seismic Engineering) founded by the Italian Civil Protection Department has presented some of the most appropriate rehabilitation techniques for these kind of structures (WG-AGI, 2012). Foundations are an integral part of the overall rehabilitation strategy and cannot be ignored during the evaluation of the overall performance of the building. Despite this, it is important to point out that reinforcement of the foundation generally takes much time, is expensive and is rather critical due to various restrictions (existing utilities, vibrations and space limits).

In the following, the most effective measures for the rehabilitation of the shallow foundations of damaged industrial buildings are presented:

Figure 51a shows the increasing of the passive resistance of the soil adjacent to existing footings. To this purpose, the in place existing soil adjacent to the existing footing may be injected with chemical grouts. Holes must be drilled through the existing grade slab to a depth from 30 to 40 cm below the pavement surface. Holes diameter must match grout injecting equipment fitting. If injections in pressure are used, the technique requires careful control to avoid causing of uplifting of the grade slab. Figure 51b shows the improvement of the frictional resistance at the base of footings. To this purpose the prefabricated footing may be connected to the sub-foundation by means of anchor bolts at the footing corners.
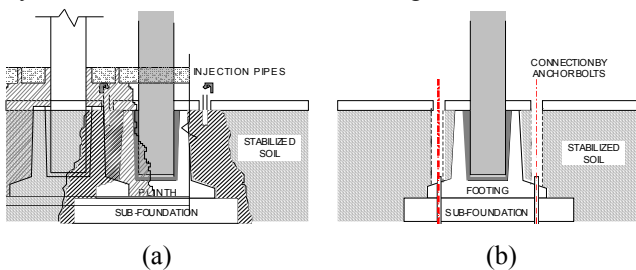

Figure 51: a) Increase of the passive resistance of the soil adjacent to existing footings; b) Improvement of the frictional resistance at the base of footings.

Figure 52 shows mitigation of differential horizontal and/or vertical displacements. In order to mitigate differential horizontal displacements, which are the most frequent during seismic events, a suitable restraint between existing columns and existing reinforced industrial pavement may be provided. An example of connection between an external column and the industrial pavement is reported in Figure 52. Alternatively, traditional cross-connection elements, such as connecting beams, tie rods, etc., can be used. In particular, connecting beams of adequate flexural rigidity, are useful for mitigating not only differential horizontal displacements but also differential vertical displacements.
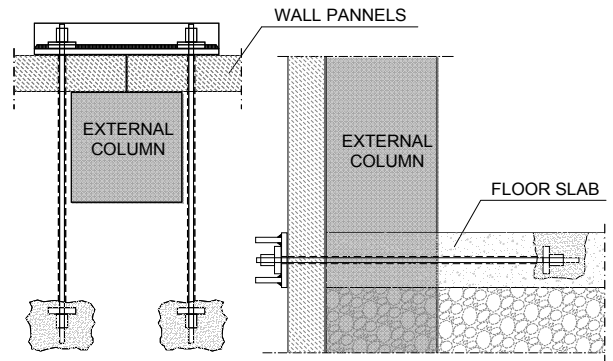

Figure 52. Connection between an external column and the industrial pavement.

The existing bending capacity of the footing must be checked. If the bearing capacity is not lack, the existing foundation must be enlarged, to increase the bearing capacity and to decrease the uplifting. It is standard practice to connect the new reinforced foundation by a number of bars drilled all the way through the existing footing. To install the longer bars, an over excavation of the adjacent soil is usually needed. The shear transfer between the new and the existing footings can be obtained by roughening the existing footing lateral faces. The existing grade slab must be partially removed, then a trench adjacent to the existing footing excavated, drilled dowels installed, rebar laid and concrete placed. This is all time-consuming, messy, and noisy.

Figure 53 shows the existing foundation improvement with additional piling and with a new footing surrounded to it. This may be effective in resisting lateral loading and in increasing compression capacity of the existing footing and to offer tension capacity. Resistance is shared between the two different elements, depending on their relative rigidity. The overall strength depends on both the soil and the structural pile capacity, including the pipe, grout, and reinforcing bar. Compression stiffness considers the pile elements and surrounding soil movement. Micropiles give uplift resistance. Structural tension strength is lower than the compression one and is due to the steel pipe only. Adequate clearance must be available for the equipment used to install micropiles inside existing buildings. This technique is time-consuming, messy, and noisy.
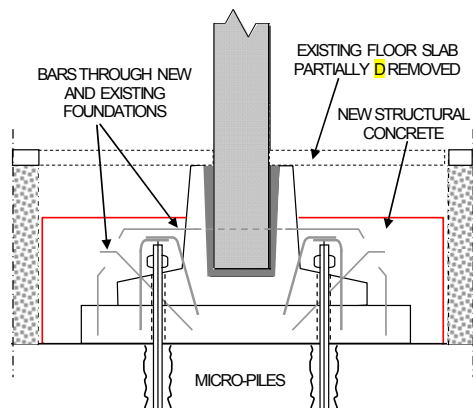
Figure 53. Existing foundation improvement with additional piling and a new footing surrounded to it.

All the previous mentioned rehabilitation measures can be performed reducing the design seismic action of 40%, according to a post-earthquake Italian Regulation (DL. 6.VI.2012, No. 74). Alternatively, the possibility of building a new foundation system around the existing one can be taken into account. The new foundation system will support a new building roof. The advantage of realizing a new foundation system around the existing one consists in avoiding the interruption of the industrial activity in the industrial building. However, in this last case the new foundation system has to be designed considering the whole design seismic action.

Finally, when loss of bearing capacity due to liquefaction and large ground displacements are expected, then soil improvements should be also considered to prevent/limit the development of excess pore water pressure and/or shear strains and vertical strains in the ground.

The soil improvements against liquefaction could be achieved by performing direct and indirect measures. The direct measures are those which increase the mechanical soil properties, such as: relative density increasing or grains cementation; the indirect measures are those which do not increase the shear strength of the soil, but decrease the consequence of liquefaction if it will occur again. Key factors to choose between direct and indirect measures are: grain size, permeability, stratigraphic profile, thickness of liquefiable soil and depth of it below the ground surface, increasing of mechanical soil properties which should be reached, vibration induced by the measures techniques, cost of the measures against liquefaction.

The criteria for design the measures against liquefaction must be: (i) increasing of cyclic soil resistance to avoid the occurrence of liquefaction for an earthquake similar to that happened on 20 and 29 May 2012; (ii) minimizing the environmental impact; (iii) minimizing the un-desired effects on the built area; (iv) minimizing the soil volume to be treated; (v) minimizing the modification of the water table regime.

For the damaged areas by the 2012 Emilia Romagna earthquake, it should be recommended, among direct measures: injections with the appropriated permeable mixtures and compaction injections; among the indirect measures: induced partial saturation on the soil and drainage.

CONCLUSION

On May 20, 2012 an earthquake of magnitude M_L=5.9 struck the Emilia Romagna Region of Italy and a little portion of Lombardia Region. Successive earthquakes occurred on May 29, 2012 with M_L=5.8 and M_L=5.3. The earthquakes caused 27 deaths, of which 13 on industrial buildings. The damage was considerable. 12,000 buildings were severely damaged; big damages occurred also to monuments and cultural heritage of Italy, causing the collapse of 147 campaniles. The very famous Finale Emilia campanile collapsed; the Mirandola Tower was severely damaged, as well as many others campaniles.

The damage is estimated in about 5-6 billions of euro. To the damage caused to people and buildings, must be summed the indirect damage due to loss of industrial production and to the impossibility to operate for several months. The indirect damage could be bigger than the direct damage caused by the earthquake.

The macroseismic survey shows heavy damage in spite of the moderate magnitude mainly due to the fact that the Emilia Romagna Region was declared seismic area starting only from 2003.

It is important to stress that the industrial buildings built after that the Region was declared seismic area in 2003, were practically not suffered any damage, even if the recorded acceleration was greater than that predicted by the Italian Regulation (NTC, 2008), equal to 0.10-0.15g with a probability of occurrence less than 10% in 50 years.

The May 20, 2012 earthquake, with M_L = 5.9 and M_w = 6.1, recorded at Mirandola, 17 km far from the epicenter, shows an horizontal acceleration of about 0.28g, while the May 29, 2012, also recorded at Mirandola, 4 km far from the epicenter, shows an horizontal acceleration of 0.22g EW and 0.29g NS; particularly severe was the vertical acceleration of 0.89g, because of the normal fault mechanism.

To investigate the geotechnical soil properties, a large series of in situ and laboratory tests and geophysical tests were performed, particularly at the damaged town of S. Carlo and Mirabello borings, piezometers, Cross Hole, piezocones and seismic piezocones were performed; laboratory resonant column tests were also performed.

The ground model for performing a preliminary site response analysis was based on the geotechnical data base of the Emilia-Romagna Regional Government (RER-DB), the geotechnical reports performed for the design of local infrastructures, especially the Cispadana highway (CIS) and by the specific in situ and laboratory tests (WG-DPC), performed after the earthquake at Sant'Agostino and Mirabello municipalities.

While the maximum site amplification was of about 1.5, the design spectra reach the maximum value of 0.70g for horizontal acceleration.

Significant and widespread liquefaction effects, which caused panic of inhabitants and damage to buildings and infrastructures, were observed in various areas of Emilia-Romagna region. More important and widespread damages resulted for buried lifelines (gas and water pipelines). The

analysis results in terms of Liquefaction Potential Index (LPI) do not seem to fully explain the great diffusion and extension of the liquefaction effects observed at San Carlo and Mirabello during the ground shaking of 20th May. Therefore, the simplified methods for estimating the liquefaction hazard seem to require a refinement in order to obtain quantitatively reliable results for regional seismic conditions.

Many industrial buildings collapsed or suffered great damage during the seismic events; this caused enormous problems to the industrial activity, which is among the most profitable of Italy in the region.

An extensive description on geotechnical shortcomings of Emilia-Romagna industrial building foundations, reported in the recent guidelines by AGI Working Group is summarized in the paper. Criteria for the seismic improvement of foundations as well as the seismic assessment and improvement of Industrial Building shallow foundations is reported and discussed. This could be achieved by improving the foundation system and/or by improvement the soil behaviour against liquefaction by direct and indirect measures. While after the 2009 L'Aquila earthquake, the resilience of the city was immediate only for rebuilding new residential isolated buildings, in the case of the Emilia Romagna earthquake, the resilience of the damaged cities to the damage to the industrial buildings and the lifelines was very good; some industries built a smart campus to start again to operate in less of one month and structural and geotechnical guidelines were edited to start with the recovering the damaged industrial buildings.

REFERENCES

Bozorgnia Y., Campbell K.W. [2004]. The Vertical-to-Horizontal spectral ratio and tentative procedures for developing simplified V/H and vertical design spectra, Journal of Earthquake Engineering, (2004), 8(2), 175-207.

Castelli V, Bernardini F., Camassi R., Caracciolo C.H., Ercolani E., Postpischl L. [2012]. Looking for missing earthquake traces in the Ferrara-Modena plain: an update on historical seismicity. Annals of Geophysics, 55, 4, 2012; doi: 10.4401/ag-6118, pp.519-524

Cazzola, F. [1997]. La ricchezza della terra. L'agricoltura emiliana fra tradizione e innovazione. In: Storia di Italia dall'unità ad oggi. Le Regioni. L'Emilia Romagna. Giulio Einaudi Editore.

Chioccarelli E., De Luca F., Iervolino I. [2012a]. Preliminary study of Emilia (May 20th 2012) earthquake ground motion records V2.1; http://wpage.reluis.it

Chioccarelli E., De Luca F., Iervolino I. [2012b]. Preliminary study of Emilia (May 29th 2012) earthquake ground motion records V1.0; http://wpage.unina.it/iuniervo/papers/Peak_Parameters_Emilia_May_29th_V1.0

D.A.L. [2007] Deliberazione dell'Assemblea Legislativa della Regione Emilia-Romagna n.112 del 2/5/2007: Approvazione dell'atto di indirizzo e coordinamento tecnico ai sensi dell'art.16 comma 1, della L.R. 20/2000 per "Indirizzi per gli studi di microzonazione sismica in Emilia-Romagna per la pianificazione territoriale e urbanistica". Boll. Uff. Reg. Emilia-Romagna n. 64 del 17/05/2007. http://demetra.regione.emilia-romagna.it/ o http://www.regione.emilia-romagna.it/geologia/

D.L. 6.VI.2012, No. 74. [2012]. "Interventi urgenti in favore delle popolazioni colpite dagli eventi sismici che hanno interessato il territorio delle province di Bologna, Modena, Ferrara, Mantova, Reggio Emilia e Rovigo, il 20 e il 29 maggio 2012". 12G0096. GU No.131, 7-VI-2012.

EC8 [2003]. Eurocode 8: Design of Structures for Earthquake Resistance - Part 1: General Rules, Seismic Actions and Rules for Buildings. December 2003.

Fioravante, V., Jamiolkowski, M. & Lo Presti, D.C.F. [1994]. Stiffness of carbonate Quiou sand. XIII ICSMFE 1994 New Delhi, India, pp. 163-167. http://www.cslp.it/cslp/index.php?option=com_content&task=view&id=66&Itemid=20

Idriss, I.M. and Sun, J.I. [1992]. SHAKE91: A computer program for conducting equivalent linear seismic response analyses of horizontally layered soil deposits. User's Guide, University of California, Davis, California.

Iwasaki T., Tatsuoka F., Tokida K.-I., Yasuda S. [1978]. A practical method for assessing soil liquefaction potential based on case studies at various sites in Japan, Proc., 2nd Int. Conf. Microzonation, National Science Foundation, Washington, DC, 885–896

Jamiolkowski, M., Lancellotta, R., Tordella, M.L. e Battaglio, M. [1982]. Undrained strength from CPT. Proceedings Esopt II, Amsterdam.

Lancellotta, R. [1983]. Analisi di affidabilità in ingegneria geotecnica. Atti Istituto Scienza delle Costruzioni n. 625. Politecnico di Torino.

Lanzo G., Pagliaroli A. [2012]. Seismic site effects at near-fault strong-motion stations along the Aterno River Valley during the Mw=6.3 L'Aquila Earthquake. Soil Dynamics and Earthquake Engineering, Vol. 40, pp. 1-14, September 2012, DOI: 10.1016/j.soildyn.2012.04.004

Liberatore L., Sorrentino L., Liberatore L., Decanini L.D. [2012]. Failure of Modern Structures Induced by the Emilia (Italy) 2012 Earthquakes. Engineering Failure Analysis (submitted).

Liquefaction resistance of soils: Summary report from the

1996 NCEER and 1998 NCEER/NSF workshops on evaluation of liquefaction resistance of soils. Jour. Geotech. Geoenviron. Eng., 127(10), pp. 817–833.

Lunne, T., Robertson, P.K. and Powell, J.J.M. [1997] Cone Penetration Testing in Geotechnical Practice, Blackie Academic/Routledge Publishing, New York.

Martelli, L. [2012]. Liquefaction effects observed in occasion of the 2012 May 20 earthquake in the Emila plane", 7th EUREGEO, Bologna, Italy.

Maugeri M., Simonelli A.L., Ferraro A., Grasso S., Penna A. [2011]. Recorded ground motion and site effects evaluation for the April 6, 2009 L'Aquila earthquake. Bull Earthquake Eng (2011) 9, pp.157–179. DOI 10.1007/s10518-010-9239-x. ISSN: 1570-761X (print version), ISSN: 1573-1456 (electronic version).

Monaco P., Santucci De Magistris F., Grasso S., Marchetti S., Maugeri M., Totani G. [2011]. Analysis of the liquefaction phenomena in the village of Vittorito (L'Aquila). Bull Earthquake Eng (2011) 9, pp. 231–261. DOI 10.1007/s10518-010-9228-0. ISSN: 1570-761X (print version), ISSN: 1573-1456 (electronic version).

Monaco P., Totani G., Barla G., Cavallaro A., Costanzo A., D'onofrio A., Evangelista L., Foti S., Grasso S., Lanzo G., Madiai C., Maraschini M., Marchetti S., Maugeri M., Pagliaroli A., Pallara O., Penna A., Saccenti A., Santucci De Magistris F., Scasserra G., Silvestri F., Simonelli A.L., Simoni G., Tommasi P., Vannucchi G., Verrucci L. [2012]. Geotechnical Aspects of 2009 L'Aquila Earthquake. M.A. Sakr and A. Ansal (eds.), Special Topics in Advances in Earthquake Geotechnical Engineering, Geotechnical, Geological and Earthquake Engineering 16, pp. 1-66. DOI 10.1007/978-94-007-2060-2_8, © Springer Science+Business Media B.V. 2012. ISBN 978-94-007-2059-6.

NTC [2008]. Le Norme Tecniche per le Costruzioni. D.M. 14 gennaio 2008 - Ministero delle Infrastrutture e dei Trasporti. Gazzetta Ufficiale 29 (supplemento Ordinario 30).

Pacor F., Paolucci R., Iervolino I., Nicoletti M., Ameri G., Bindi D., Cauzzi C., Chioccarelli E., D'Alema E., Luzi L., Marzorati S., Massa M., Puglia R. [2009]. Strong ground motion recorded during the L'Aquila seismic sequence, Progettazione Sismica, 3, 55-67.

Pergalani F., Compagnoni M. [2012]. Studio dell'amplificazione e degli inputs sismici nei comuni classificati in zona sismica 3 lungo la sponda destra del Fiume Po delle Province di Reggio Emilia e Mantova. Relazione finale.

Pesci, A., Bonali, E. [2012]. Occhi speciali: il campanile di Mirandola dopo il terremoto del 20 e del 29 Maggio 2012 visto al laser scanning. Technical Report. (http://www.centroeedis.it/allegati/LASER%20scheda.Pesci).

Rainieri, C., Fabbrocino, G. [2011]. Predictive correlations for the estimation of the elastic period of masonry towers. EVACES 2011 - Experimental Vibration Analysis for Civil Engineering Structures, Varenna (IT) 3-5 October 2011, 2011.

Robertson P. K., Wride C. E. [1998]. Evaluating cyclic liquefaction potential using the cone penetration test. Canadian Geotechnical .Journal, 35(3), 442–459.

Robertson, P. K. [1990]. Soil classification using CPT. Canadian Geotechnical Journal, Ottawa, 27(1), pp. 151–158.

Rovida A., R. Camassi, P. Gasperini and M. Stucchi, eds. [2011]. CPTI11, Parametric Catalogue of Italian Earthquakes, 2011 version, Milano, Bologna; available online: http://emidius.mi.ingv.it/CPTI

Seed R.B., Cetin K.O., Moss R.E.S., Kammerer A.M., Wu J., Pestana J.M., Riemer M.F., Sancio R.B., Bray J.D., Kayen R.E., Faris A. [2003]. Recent advances in soil liquefaction engineering: a unified and consistent framework. Report No. EERC 2003-06, Earthquake Engineering Research Center, College of Engineering, University of California, Berkeley

Seed, H.B., Wong, R.T., Idriss, I.M., and Tokimatsu, K. (1986). Moduli and damping factors for dynamic analyses of cohesionless soils. Journal of Geotechnical Engineering, ASCE, Vol. 112, pp.1016-1032.

Severi, P. and Staffilani F. [2012]. Geologia ed Idrogeologia della pianura Ferrarese, WARB Conference, Copparo Ferrara, Italy.

Sibson, R. [1981]. A Brief Description of Natural Neighbor Interpolation, chapter 2 in "Interpolating Multivariate Data". New York: John Wiley & Sons, pp. 21–36.

Sun, J.I., Golesorkhi, R., and Seed, H.B. [1988]. Dynamic moduli and damping ratios for cohesive soils. Report No. EERC-88/15, Earthquake Engineering Research Center, University of California, Berkeley.

Toscani, G., P. Burrato, D. Di Bucci, S. Seno, G. Valensise [2009]. Plio-Quaternary tectonic evolution of the northern Apennines thrust fronts (Bologna-Ferrara section, Italy): Seismo-tectonic implications, B. Soc. Geol. Ital., 128, 605-613.

Tropeano G., Ausilio E., Costanzo A., Silvestri F. [2009]. Valutazione della stabilità sismica di pendii naturali mediante un approccio semplificato agli spostamenti. XIII Convegno Nazionale "L'Ingegneria Sismica in Italia (ANIDIS 2009)", Bologna, 28 giugno –2 luglio 2009.

Tropeano G., Silvestri F., Gazzaneo D., Ausilio E. [2012]. Parametri di intensità sismica per la stima degli spostamenti

permanenti di pendii omogenei. IARG 2012, Padova.
http://www.image.unipd.it/iarg2012/atti/

Vannucchi G., Crespellani T., Facciorusso J., Ghinelli A., Madiai C., Puliti A., Renzi S. [2012]. Soil liquefaction phenomena observed in recent seismic events in Emilia-Romagna Region, Italy. International Journal of Earthquake Engineering, Vol 2-3, Pàtron Editore, Bologna.

WG-DPC [2012]. The Emilia thrust earthquake of 20May 2012 (Norhern Italy): strong motion and geological observations. Mirandola Earthquake Working Group (Uni Chieti, Uni Trieste, Regione Umbria). Report 1.
http://www.protezionecivile.gov.it/jcms/it/ran.wp

WG-DPC [2012]. The Emilia thrust earthquake of 20May 2012 (Norhern Italy): strong motion and geological observations. Mirandola Earthquake Working Group (DPC, UniChieti, Uni Trieste, Regione Umbria) – Report 2.
http://www.protezionecivile.gov.it/jcms/it/ran.wp

WG-RELUIS [2012] Linee di indirizzo per interventi locali e globali su edifici industriali monopiano non progettati con criteri antisismici. Working Group RELUIS , Protezione Civile, Consiglio Nazionale degli Ingegneri.
http://www.reluis.it/images/stories/Linee%20di%20indirizzo%20v2_5.pdf

WG-AGI [2012]. "Linee di indirizzo per interventi su edifici industriali monopiano colpiti dal terremoto della pianura padana emiliana del maggio 2012 non progettati con criteri antisismici: aspetti geotecnici". Rapporto Gruppo di lavoro AGI per gli edifici industriali.

Youd T.L. [1998]. Personal communication to Lew M., Martin G.R. – What structural engineers need to know about liquefaction. SEAOC 1999 Convention, pp. 45-63

Youd T.L., Idriss I.M., Andrus R.D., Arango I., Castro G., Christian J. T., Dobry R., Liam Finn W. D., Harder L. F. Jr., Hynes M.E., Ishihara K., Koester J.P., Laio S.S.C., Marcuson Iii W.F., Martin G.R., Mitchell J.K., Moriwaki Y., Power M S., Robertson P.K., Seed R.B., Stokoe II K.H. [2001]. Liquefaction resistance of soils: Summary report from the 1996 NCEER and 1998 NCEER/NSF workshops on evaluation of liquefaction resistance of soils. Jour. Geotech. Geoenviron. Eng., 127(10), 817–833.